IEEE Access
Multidisciplinary | Rapid Review | Open Access Journal

Received 28 June 2024, accepted 12 July 2024, date of publication 15 July 2024, date of current version 23 July 2024.

Digital Object Identifier 10.1109/ACCESS.2024.3429028

RESEARCH ARTICLE

Interception of Signals With Very Weak SINR

ALI MANSOUR, (Senior Member, IEEE), AND CHRISTOPHE OSSWALD
Lab STIC, UMR 6285 CNRS, ENSTA Bretagne, 29200 Brest, France

Corresponding author: Ali Mansour (mansour@ieee.org)

This work was supported by the l'Agence de l'Innovation de Defense a la Direction Générale de l'Armement—Ministère des Armées (AID-DGA) and Agence Nationale de le Recherche en France (ANR) through ANR-Accompagnement Spécifique des travaux de Recherches et d'Innovation Défense (ASTRID) under Project ANR-19-ASTR-0005-03.

ABSTRACT To protect our receivers against spoofing, intrusion or simply reduce interference, we proposed a multi-layered architecture which can be integrated into a receiver chain by modifying the analog and digital parts. Indeed, Our project addresses analog circuits coupled with digital approaches to immunize a radio against any intentional electromagnetic attack (intelligent jammer or not), or radio interference. In this manuscript, we only consider the innovative analog part of our system which is based on non-linear bijective functions generated by electronic circuits. In fact, we have developed an electronic system characterized by a non-linear bijective function that can be implemented using analog electronic components, and its inverse function can be implemented in the digital part of our reception chain. The main purpose of these two functions is the protection of an interesting weak signal existing in the vicinity to an annoying but very strong signal which will risk saturating the Low Noise Amplifier (LNA), and therefore the target signal can no more be chased after the analog to digital convertor (ADC). Certainly, in conventional transmission systems, we generally seek to eliminate or to reduce the impact of non-linear effects of certain electronic components or devices; however, our proposed scheme introduce a specific non-linear function in ordre to detect the presence of signals with weak Signal to Interference plus Noise Ratios (SINR). This manuscript presents our study and discusses various aspects related to the proposed new nonlinear scheme.

INDEX TERMS Wireless networks, jamming, electronic warfare, interference, AGC, ASK, PSK, FSK, QAM, OFDM, nonlinear amplification, ADC, IoT, SDR, WLAN.

I. INTRODUCTION

The telecommunication adventure has begun with the invention of the telegraph. Telephony then appeared. We then transported the human voice in an analog way. The third industrial revolution can be related to the advent of computing and the simultaneous expansion of telecommunication. Later on, digital technology, to transport voice, image or computer data, was introduced and has been continuously evolving. As long as there is a communication channel between two users, they can exchange their data [1].

In the last three decades, mobile telephony has experienced great growth from the first generation (1G) to 5G. With the introduction of these technologies into our societies, we first observe that the number of mobile phones has increased exponentially to reach the threshold of 5 billion in 2019, then the innovation in telecommunications has been widely supported by recent civil applications to exceed strategic and military needs. In fact, ad-hoc networks (for example: Mobile Ad hoc Networks (MANET)) were mainly used for military applications; however, civil telecommunication industries have recently introduced several innovative concepts with a great acceleration, such as: Cognitive Radio, Software Defined Radio (SDR), Software Defined Networking (SDN), Visible Light Communication (VLC), Wireless Fidelity (WiFi), etc. With the arrival of the Internet of Things (IOT), we expect 3 trillion USD ($3 * 10^{12}$\$) in revenue and more than 27 billion communicating objects by the end of 2025.[1] This development will force communicating objects and other systems to intelligently share spectral resources by tolerating a lower Signal to Interference plus Noise Ratio (SINR) level and by reducing the guard margins between

The associate editor coordinating the review of this manuscript and approving it for publication was Mohamed M. A. Moustafa.

[1] According to Gartner - IOT Forecast Tool: "IOT connections will grow to 27 billion ··· with total IOT revenue opportunity will be USD 3 trillion in 2025"

different transmitters. This evidence will undoubtedly impact the complexity of our systems by creating more interference and thus increasing the fragility of communicating systems.

In the context of electronic warfare or civil surveillance, we are faced with the problem of undefined multi-component identification and recognition of digital modulations. Early work in this area was classified and discussed in [2]. In this work, Azzouz and Nandi developed statistical techniques for the recognition and characterization of classical digital modulation signals (Amplitude Shift Keying (ASK), Frequency Shift Keying (FSK) and Phase Shift Keying (PSK)). In previous studies [3] and [4], we extended the work of Azzouz and Nandi. While additionally considering Quadrature Amplitude Modulation (QAM) signals, Pinet [5] carried out the recognition and characterization of classical digital modulation signals by applying certain modified statistical functions on time-frequency representations (TFR) of observed signals. Other modified statistical functions applied on TFR of the observed signals were developed in [6], [7], and [8]. More statistical tools have been proposed in [9] and [10].

In wireless communications, the bandwidths for uplink or downlink are relatively wide, and the bandwidth allocated for the downlink is generally greater than the one reserved for the uplink. The bandwidth defines the capacity of the network, which must allow multiple uses, including high-speed services. Particularly uplink signals transmitted by different terminals often contain multiple components of very high amplitudes. The reception of such signals requires the design of a receiver with the capacity to handle large amplitude dynamics. The significant amplitude dynamics are generally proportional to the dynamics of the signal-to-interference-plus–noise ratio (SINR).

In an electronic warfare or a simply signal surveillance, we can face a huge challenge to detect and process a weak received signal, where its bandwidth is adjacent to the bandwidth of a strong jammer or broadcasting signals. The basic idea is then to reduce the strong level signals in order to decrease the total amplitude dynamics in a target bandwidth, without affecting much the performance at the processing output. Two approaches are possible:

1) Reduce the level of the strong interfering signal by applying a notch filter at the beginning of the reception chain,
2) Introducing a logarithmical amplifier, that can bounded the strong signal level at the input of the reception chain. In this case, the received signal composed of the strong interference signal and a weak target signal can to be straightforward sampled using a conventional analog/digital converter (ADC).

It is worth mentioning that most of current receivers, civil or military, are digital. In these devices, an analog signal, digitally modulated, is transmitted using a radio wave, then picked up by the antenna of the digital receiver. It undergoes several transformations and processing in order to extract the transmitted information [11], [12], [13]. These processing steps, which are necessary for the reception, can be harmful or ineffective if the transmitted signals do not respect the protocols of the network [14]. Hereinafter, we focus on the case of "an intentional jammer wants to harm a receiver". This jammer may not respect the communication rules in the targeted network and that it thus generates a powerful harmful signal which may be in the spectral band of the legitimate signal (in this scenario, the jammer has a priori information on the network) or just nearby (if the jammer is not intentional, a radio or television transmitter for example, or if the transmitted signal is a broadband signal of type Direct-Sequence Spread Spectrum (DSSS) or Frequency Hopping Spread Spectrum (FHSS) [15].

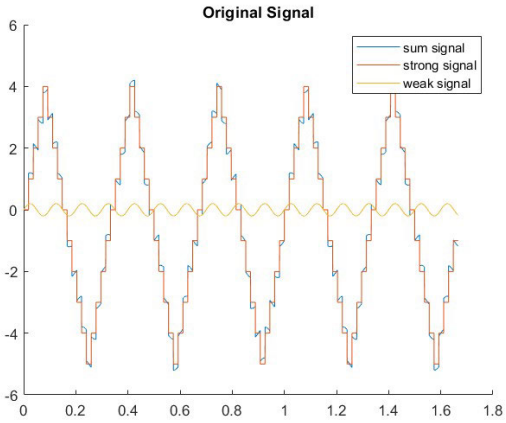

FIGURE 1. Received signals.

To clarify the context and explain our main idea, we consider the scenario; where the received signals can be written as follows:

$$y(t) = x(t) + s(t) + n(t),$$

$x(t)$ is the strong jamming signal, $s(t)$ represents the weak signal of interest, and $n(t)$ stands for an additive white gaussian noise (AWGN). The three signals are illustrated in Fig. 1.

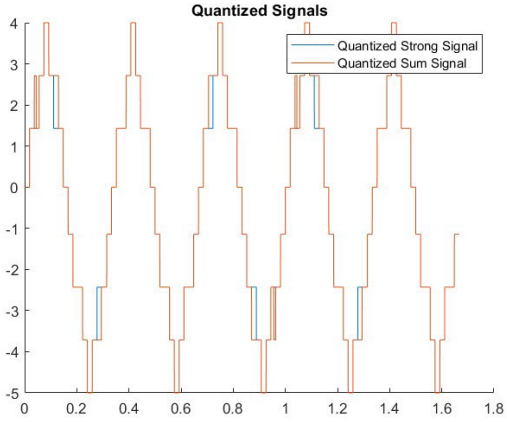

FIGURE 2. Quantized signals.

By applying a quantization procedure, it can be shown that weak signals can be largely affected by this procedure. Indeed, the signature of these signals in the digital part can be negligible or even non-existent, specially after a Radio Frequency (RF) matched filter and an Automatic Gain Control (AGC). Fig. 2 illustrates the effect of quantization; where we can clearly notice that the observed quantized signal becomes almost the strong quantized signal. To solve this issue and protect the useful low-power signal, we introduce a bijective non-linear function $\Phi()$ at the input of the reception chain. This saturation function can amplify low amplitudes while bounding signals with higher amplitudes. Once the distorted signal has passed through the analog/digital converter (ADC), an inverse function should be applied. This procedure can thus keep part of the faint signal, allow the detection of such signals or recover its information, see Fig. 3. The non-linear function $\Phi()$ must be invertible and similar to a sigmoid function. Several functions can be candidates, such as: arctan, log, tanh, etc. The chosen function must be achievable by an analog electronic circuit.

FIGURE 3. The concept of receiver with high amplitude dynamics.

II. RECEPTION CHAIN

A generic and universel receiver does not exist, and based on different references [16], [17], [18], [19], [20], we propose a typical complete system whose components are the most used in various receivers. Fig. 4 shows a general diagram of a typical receiver with its most frequently used components in modern systems:

- The receiver chain starts by the antenna and its characteristics (gain, frequency band, radiation lobes, beam widths, geometric shape, etc.).
- A radio frequency filter: ''RF/Matched Filter'' centered on the frequency band of interest. This filter can be a classic or an adaptive one, or also an anti-InterSymbol interference (ISI) filter (such as the filter raised cosine filter[2]).
- A mixer used with a local oscillator (LO) to eliminate the carrier and regenerate a baseband or intermediate frequency signal (IF).
- A second bandpass filter can eliminate the high frequencies produced by the mixer.
- An automatic gain control (AGC) protects the chain from overvoltage and reduces saturations in the recovered signal.
- An analog-digital converter (ADC) [20], [21] consists mainly of the following sub-circuits:
  - An anti-aliasing filter.
  - A sampler.
  - A uniform quantifier.
- A digital processing component allows the signal to be demodulated and the information to be extracted. This component depends on the type of modulation and the network protocol used. Generally, four subcomponents can be found:
  - A channel equalizer to reduce the effect of the transmit channel.
  - A demodulator.
  - A channel decoder to correct transmission errors and reduce the bit error rate (BER).
  - A source decoder to decompress the signal.

[2]A raised cosine filter, with a roll-off-factor β, has the following transfer function:

$$X_{RC}(f) = \begin{cases} T & |f| \leq \frac{1-\beta}{2T} \\ \frac{T}{2}\left(1+\cos\left(\frac{\pi T}{\beta}(|f|-\frac{1-\beta}{2T})\right)\right) & \frac{1-\beta}{2T} \leq |f| \leq \frac{1+\beta}{2T} \\ 0 & |f| > \frac{1+\beta}{2T} \end{cases}$$

III. ADC ISSUES

An analog-to-digital converter (ADC) is mainly equivalent to two steps: sampling and quantization. The quantization involves presenting a continuous interval with a limited number of distinct code words, input values are therefore rounded to the nearest output values. Several kinds of issues can thus interfere with the conversion process. For example, sample rate and resolution can be a big problem. Real ADC have several types of unwanted nonlinearities. Gain and offset errors are important but their effects are fairly trivial to mitigate. Other nonlinearities are differential nonlinearities (DNL) and integral nonlinearities (INL).

Quantization undeniably induces a loss of information, and even in the ideal case, it is a non-linear operation linked to the input range of the ADC. If the input range consists of only positive voltages, the quantization is said to be unipolar. Similarly, an input range with both positive and negative voltages corresponds to a bipolar quantizer. The quantization thresholds should not be evenly spaced. For example, in some applications, values close to zero may be more important than large values. While keeping the number of bits constant, for low values resolution can be increased at the expense of precision in large values using non-uniform quantizer. The loss of information due to a finite word length is called quantization noise. It can be conveniently expressed with a quantization signal-to-noise ratio (SQNR). Hereinafter, we discuss different classical operations used in an ADC and their impacts on the observed signal spectra.

A. LIMITED OBSERVATION PERIOD

This is a classic problem in signal processing linked to the definition of the continuous or discrete Fourier transform. A quick illustration of this problem will subsequently allow us to better understand the other phenomena presented in our

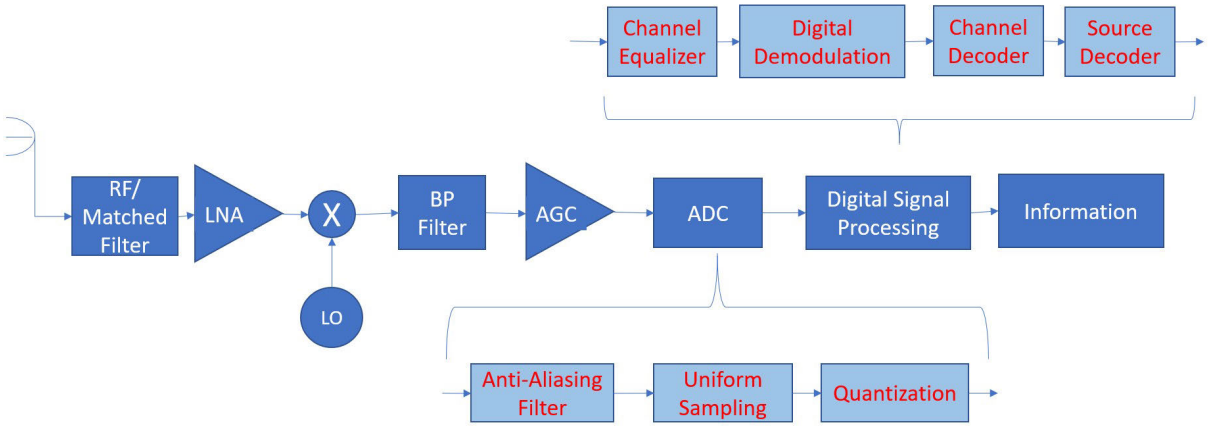

FIGURE 4. A typical schematic of a digital receiver: Automatic Gain Control (AGC), Analog to Digital Convertor (ADC), Local Oscillator (LO) and Band-pass filter (BP filter).

results. To clearly illustrate this problem, we first recall the definition of the Fourier transform, $X(f)$ of a continuous real signal $x(t)$:

$$X(f) = \int_{-\infty}^{\infty} x(t) \exp(-j\,2\pi f t)\, dt \tag{1}$$

where j is the complex number and f stands for the frequency. So, the integral should be carried out over the entire time axis; which is not possible in real world applications. Considering that our signals are causal, i.e. $\forall t < 0 \rightarrow x(t) = 0$, this cannot completely resolve a practical problem linked to the observation time, T, of a real signal, since we know well that our observations are limited in time. This limitation can be modeled as follows:

$$y(t) = x(t) w_T(t) \xrightarrow{\text{TF}} Y(f) = X(f) * W_T(f) \tag{2}$$

with T is the observation time, $w_T(t)$ represents a weighting window of duration T, $\xrightarrow{\text{TF}}$ stands for the Fourier transform, $Y(f) = TF(y(t))$, $W_T(f) = TF(w(t))$ and $*$ is the convolution product. Knowing that:

$$x(t) = \cos(2\pi f_0 t) \Rightarrow X(f) = \frac{\delta(f - f_0) + \delta(f + f_0)}{2}$$

$$w_T(t) = \begin{cases} 1 \ \forall t \in [0, T] \\ 0 \quad \text{if not} \end{cases} \Rightarrow$$

$$W_T(f) = T \exp(-j\pi f T) \text{sinc}(\pi f T)$$

with $w_T(t)$ is a rectangular weighting (or observation) window, $sinc(x) = \frac{\sin(x)}{x}$ is the cardinal sine function, and $\delta()$ is the Dirac impulse. Based on the last equation, the properties of the convolution product, and the Dirac impulse, we can then show that:

$$|Y(f)| = T \frac{\text{sinc}(f - f_0) + \text{sinc}(f + f_0)}{2} \tag{3}$$

Therefore, the main-lobe width of the observed signal $y(t)$ is equal to $\frac{2}{T}$ and it is twice the width of the secondary lobes. The ratio between the maximum amplitudes of the main lobe and the first side lobes is given by $1.5\pi \approx 4.7$, these results can be verified in Fig. 5. Indeed, in this figure, we can no longer observe the Dirac which theoretically must be the spectrum of the signal in the positive frequency domain; but we find the signature of the sinc function.

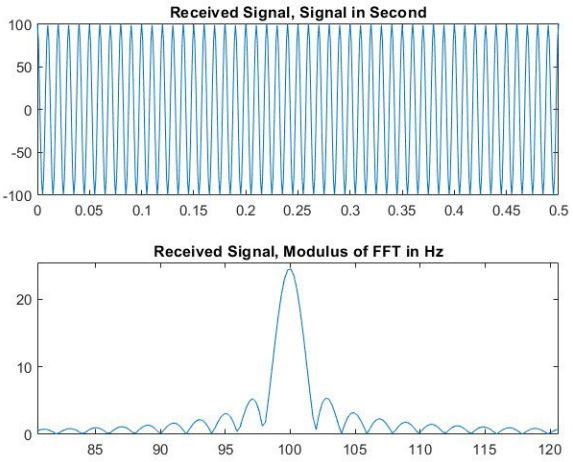

FIGURE 5. The spectrum of sinusoidal signal with limited observation period.

B. SAMPLING

Sampling is a classic and well-known procedure in digital signal processing. The sampling of a continuous signal $x(t)$ can be considered as the result of a product between this signal and a Dirac comb $e_{T_s}(t)$:

$$x_s(t) = x(t) e_{T_s}(t) = x(t) \sum_{n \in \mathbb{Z}} \delta(t - nT_s)$$

$$= \sum_{n \in \mathbb{Z}} x(nT_s) \delta(t - nT_s) \tag{4}$$

here $\mathbb{Z}$ is the set of relative integers, $F_s = \frac{1}{T_s}$ is the sampling frequency, T_s is the sampling period. By applying the Fourier

transform, we can then write:

$$X_s(f) = X(f) * E_{T_s}(f) = \frac{1}{T_s} X(f) * \sum_{n\in\mathbb{Z}} \delta(f - nF_s)$$
$$= F_s \sum_{n\in\mathbb{Z}} X(f - nF_s) \quad (5)$$

here $E_{T_s}(f) = TF(e_{T_s}(t))$ is the Fourier transform of the Dirac comb. To find $E_{T_s}(f)$, we use a Fourier series decomposition. According to the last equation, we notice that sampling becomes equivalent to a periodization operation. This last operation explains that the minimum sampling frequency (Nyquist theorem) must be twice as large as the maximum frequency of the signal. Hereinafter, we assume that our system respects the Nyquist theorem to avoid any aliasing problem.

C. QUANTIZATION

Quantization can be considered as an injection between a real interval $[V_{\min}, V_{\max}]$ limited by the min and max values of a real sampled signal $x(k)$ to a set of 2^N distinct values, where N represents the number of quantization bits. The quantization step, q, is the value between two successive quantized values:

$$q = \frac{V_{max} - V_{min}}{2^N - 1} \quad (6)$$

The quantization noise on each sample can be presented as an additive noise:

$$x_q(k) = x(k) + n(k) \quad (7)$$

with k is the discrete time, $x(k)$ and $x_q(k)$ are the sampled and quantized signal respectively. Depending on the value of $x(k)$, $V_{\min}$, $V_{\max}$ and N, the sample of $n(k)$ can take any value from the interval $[-\frac{q}{2}, \frac{q}{2}]$. In this case, the noise $n(k)$ can be modeled by a uniform zero-mean random variable in $[-\frac{q}{2}, \frac{q}{2}]$ with its standard deviation σ_n:

$$E\{n(k)\} = 0$$
$$\sigma_n^2 = E\left\{n^2(k)\right\} - (E\{n(k)\})^2$$
$$= \frac{1}{q}\int_{-\frac{q}{2}}^{\frac{q}{2}} n^2 dn = \frac{q^2}{12} \quad (8)$$

According to equation (7), the spectrum of a quantized signal, $X_q(f) = \mathrm{TF}(x_q(k))$,[3] is equal to the spectrum of the original signal, $X(f) = \mathrm{TF}(x(k))$, but polluted by a much wider background noise in the frequency band whose power can be determined by equation (8).

To clearly illustrate the idea that the quantization procedure widens the spectrum of a quantized signal, let us consider the case of a sinusoidal signal shown in Fig. 6 with its quantized version. Fig. 7 presents the spectrum of the signal considered.

The quantization of a sinusoidal signal generates a periodic signal (see Fig. 6) which can therefore be decomposed into Fourier series with a fundamental frequency and multiple harmonics. In Fig. 8, we can observe the appearance of the 3rd harmonic. To properly illustrate this phenomenon, it is necessary to adapt the sampling frequency. Indeed, according to Nyquist's theorem, the sampling frequency of the signal illustrated in Fig. 5 must be greater than 200 Hz. Considering the effect of quantization, this frequency must be increased to over 600 Hz to properly observe the 3rd harmonic and much more to illustrate the higher harmonics, see Fig. 8.

[3]Here, TF represents a discrete Fourier transform in time, with a discrete frequency, $X_q(m)$ or continuous frequency $X_q(f)$.

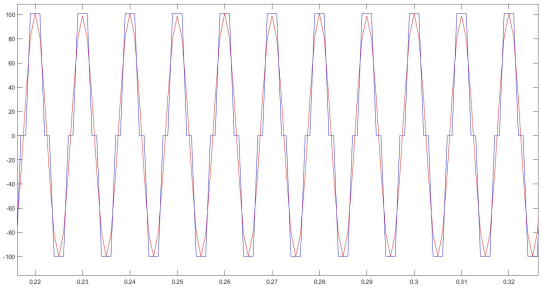

FIGURE 6. Sinusoidal signal and its quantized version.

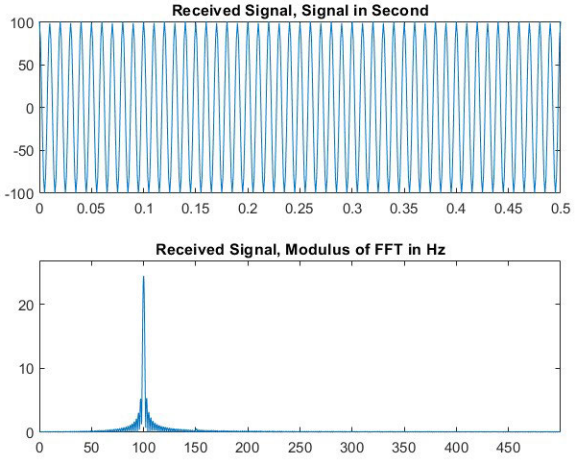

FIGURE 7. Sinusoidal signal and its spectrum.

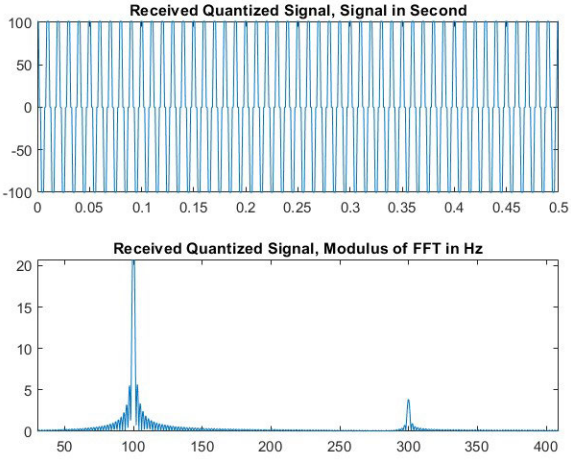

FIGURE 8. Spectrum of a quantized sinusoidal signal.

IV. INTEREST OF NON-LINEAR AMPLIFICATION

In the previous section, we discussed the effects of an analog-to-digital converter (ADC) on the digital signal and its spectrum. In this section, we consider an observation signal, $x(t)$, formed by the sum of two signals according to the following model:

$$x(t) = \alpha s(t) + \beta i(t) + n(t) \tag{9}$$

where $s(t)$, $i(t)$ and $n(t)$ are respectively the signal of interest, the interference (or jammer) signal and the additive noise of the transmission channel. Without any loss of generality, we consider that $s(t)$, $i(t)$ are normalized with unit power; but α and β are two power factors to adjust the signal to interference and noise ratio (SINR). Hereinafter, In the remainder of this section we consider that $\beta \gg \alpha$. In addition, we can assume that the extreme amplitudes, $V_{\max}$ and $V_{\min}$, of the signal $x(t)$ are given by the following equation:

$$V_{\max} = -V_{\min} = \alpha + \beta + \max(n(t)) \approx \alpha \tag{10}$$

Here, we assume a good SNR and that the signals are more or less zero mean. In this case and according to equation (6), the quantization step becomes:

$$q \approx \frac{\beta - (-\beta)}{2^N - 1} \approx 2^{1-N}\beta \tag{11}$$

If $\alpha < 2^{1-N}\beta$ then the signal $s(t)$ becomes insignificant without any influence on the quantized signal. According to the last equation and equation (8), the variance of the quantization noise becomes:

$$\sigma_n^2 \approx \frac{1}{3}\left(\frac{\alpha}{2^N}\right)^2 \tag{12}$$

The SNR becomes:

$$\text{SNR} \approx \frac{\alpha^2 + \beta^2}{\sigma_n^2 + \frac{\beta^2}{3*4^N}} \tag{13}$$

In addition, the SINR becomes:

$$\text{SINR} \approx \frac{\alpha^2}{\beta^2 + \sigma_n^2 + \frac{\beta^2}{3*4^N}} \tag{14}$$

To show the interest of a non-linear procedure necessary for the detection of a weak signal drowned out by a strong interference signal, we carried out several simulations by varying:

- The signal-to-noise ratio (SNR).
- The ratio between α and β therefore SINR.
- The number of bits used in the quantizing N.
- The nature of the signals $s(t)$ and $i(t)$.
- The non-linear function and its parameters $\Phi()$.
- The choice of the weak signal recovery bandpass filter and its characteristics (type, cutoff frequencies, order, etc.)
- The frequency bands of $s(t)$ and $i(t)$, δ_f and the offset, Δ_f, between the central frequencies of $s(t)$ and $i(t)$.

Our simulations show the impact of the different options. They also confirmed the effects previously discussed and the importance for the choice of the function $\Phi()$. The two subsections IV-B and IV-C analyze two different scenarios.

It should be noted that the "Ideal Situation" phase can only be suitable for analog receivers and we use these signals in our simulations.

A. CHOICE OF NON-LINEAR FUNCTION

As mentioned above, several non-linear functions, $\Phi()$, can be considered in our processing chain such as: square root, tangent, hyperbolic tangent, sigmoid, etc. The choice of the non-linear function can thus affect the number of harmonics and the limitation of the α/β ratio. We have thus tested several non-linear functions. Certain functions such as the hyperbolic tangent can quickly reach its saturation. Indeed, by applying the function tanh to the sum of two simple sinusoidal signals, we observed a square signal as can be verified in Fig. 10, where we can observe the square signal and all its harmonics in the spectrum.

To limit the saturation effect observed in the hyperbolic tangent function and the harmonics thus obtained, we generated another non-linear function:

$$y = \Phi(x) = \begin{cases} x & \text{If } |x| \leq 1 \\ \text{Sgn}(x)\,(\log(|x|) + 1) & \text{Elsewhere} \end{cases}$$

$$x = \Phi^{-1}(y) = \begin{cases} y & \text{If } |y| \leq 1 \\ \text{Sgn}(y)\exp(|y| - 1) & \text{Elsewhere} \end{cases}$$

where Sgn stands for the sign function[4].

To amplify the linear part and further reduce the saturated part, we then developed another non-linear function:

$$y = \Phi(x) = \begin{cases} x & \text{iff } \gamma|x| \leq 1 \\ \text{Sgn}(x)\,(\log(|x|) + \gamma) & \text{Elsewhere} \end{cases}$$

$$x = \Phi^{-1}(y) = \begin{cases} y/\gamma & \text{If } |y| \leq \gamma \\ \text{Sgn}(y)10^{(|y|-1)} & \text{Ifnot} \end{cases}$$

where $\gamma \geq 1$ is a control parameter.

It worth mentioning that the developed non-linear functions must be invertible to carry out the inversion in the digital part: they must therefore be bijective. Certain non-linear functions such as the square root, which is a bijective function for positive real signals, becomes non-bijective for signals admitting negative values. In this case, we can replace the square root function $y(t) = \sqrt{x(t)}$ by another function like $y(t) = Sgn(x(t))\sqrt{|x(t)|}$ or complete with another non-linear function for negative values. These functions must also have a certain continuity and derivability to reduce the discontinuities of the signals, which will not be well managed at the physical level, and thus reduce the harmonic components. Last important property of these functions: they must be achievable using electronic components or analog circuits.

[4] $\text{Sgn}(x) = \begin{cases} 1 & \text{If } x \geq 0 \\ -1 & \text{If } x < 0 \end{cases}$

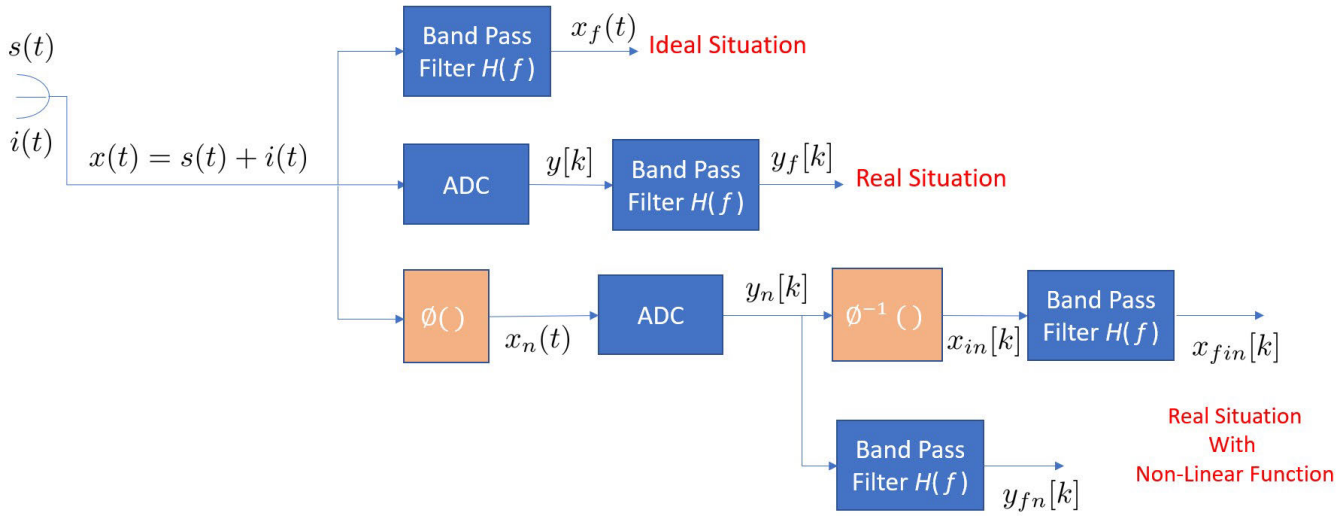

FIGURE 9. Three simulation options.

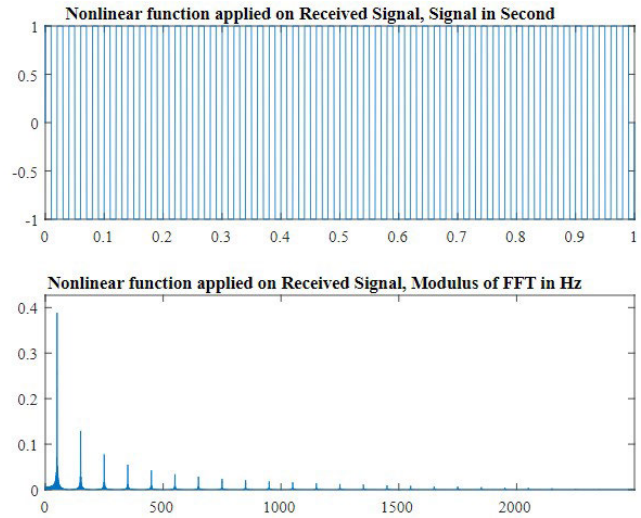

FIGURE 10. The saturation observed by applying tanh to the sum of two simple sinusoidal signals.

B. BASIC SIGNALS

To clarify our ideas and illustre certain aspects discussed above, we consider in this simulation a simple case based on equation (9) and the signal shown in Fig. 9, with:

- The observation duration is 0.5 seconds,
- The interfering signal $i(t) = \cos(200\pi t)$, where t is measured in seconds,
- The signal of interest is $s(t) = \cos(340\pi t)$,
- $\alpha = 1$ and $\beta = 100$, which results in a ratio of 40dB between the two signals, so the signal of interest is completely drowned out by the jammer signal $i(t)$.

Fig. 13 shows that the target signal $s(t)$ is almost non-existent. Indeed, by zooming in on the frequency of the signal $f = 170$Hz then we can hardly notice the spectrum of the signal $S(f)$, see Fig. 14.

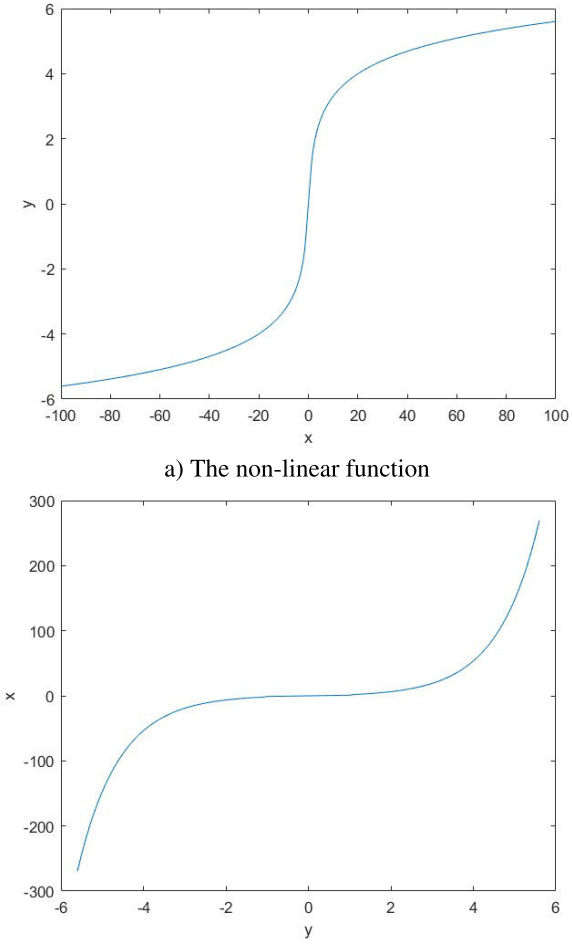

a) The non-linear function

b) Its Inverse.

FIGURE 11. A non linear function that can suppress undesired harmonics.

Concerning the sampling frequency, $f_s = 2$KHz, we chose in this simulation a f_s much greater than the threshold fixed by

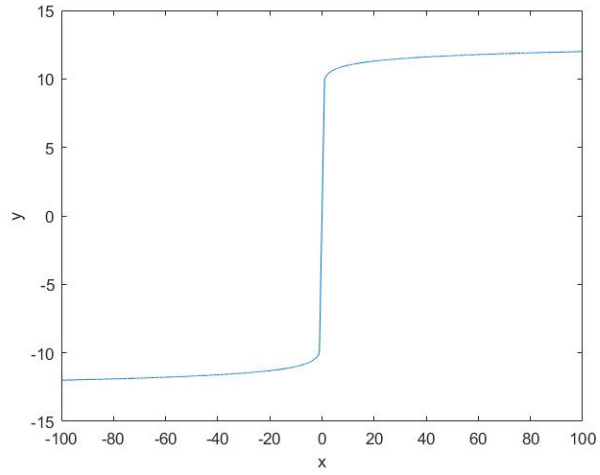

a) Another candidate for nonlinear function

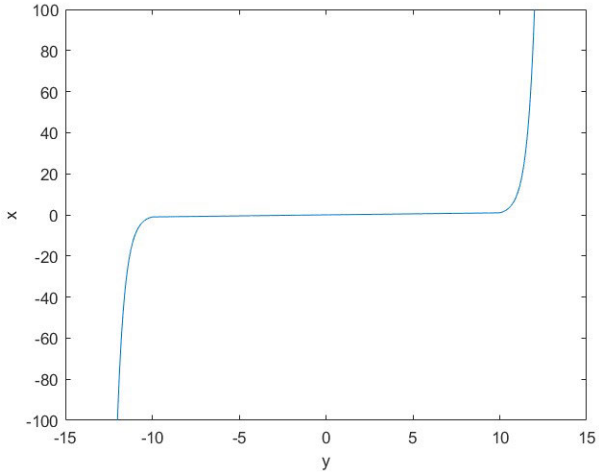

b) its inverse.

FIGURE 12. A non-linear function used in our simulations.

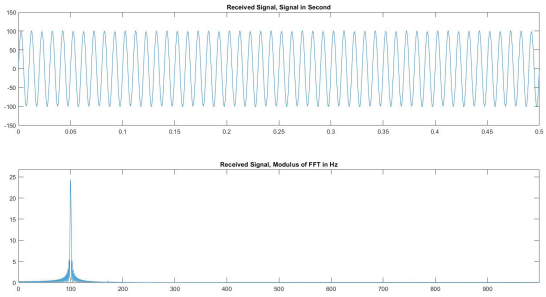

FIGURE 13. The observed signal $x(t)$ and its spectrum $X(f)$.

the Nyquist sampling theorem, $\approx$ 350Hz, to take into account certain harmonic frequencies. To highlight the quantization problem, we can select $N \approx 6$. To better illustrate these effects, we minimized $N = 2$ as much as possible so that the interfering signal keeps its characteristics and the target signal almost disappears at the analog-to-digital converter output.

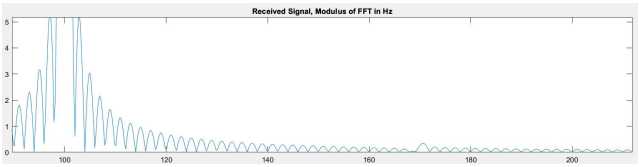

FIGURE 14. The spectrum $X(f)$ of the observed signal around $f = 170$Hz.

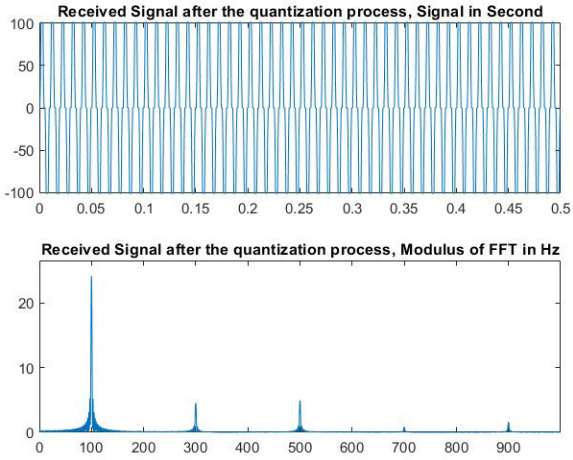

FIGURE 15. The quantized signal $y[k]$ and its spectrum $Y[m]$.

In Fig. 15, we can notice that the weak signal has completely disappeared and we also see the harmonics of the main signal. To recover the target signal $s(t)$, we implemented a "Butterworth" bandpass filter,[5] of order 6, with its cutoff frequencies $f_{c1} = 150$Hz and $f_{c2} = 200$Hz.

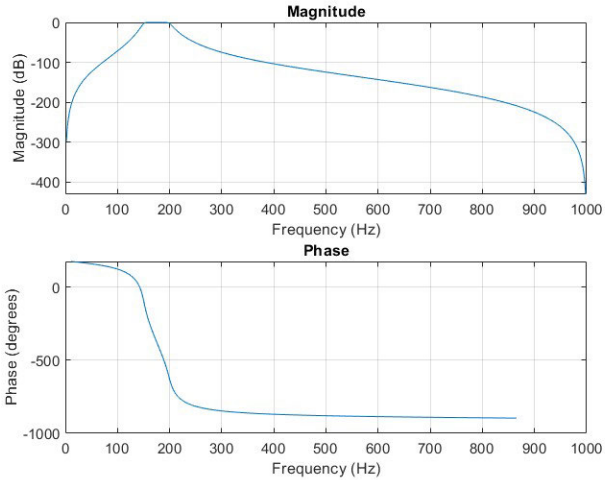

FIGURE 16. The amplitude and phase of the bandpass filter, $H(f)$, centered on the spectrum of the useful signal.

[5]In our simulations, we tried various filters with different orders and parameters. The results obtained by the Butterworth filter were very good. So, we carried out several simulations with different orders and we observed good results with orders greater than 4. On the other hand, for certain scenarios and signals, we observed certain cases of divergence with an order ≥ 8 . We thus select the order 6 with this type of filter.

To show the effectiveness of the filter, $H(f)$, we applied it on the received signal $x(t)$ in an ideal context (i.e. the ''ideal situation'' phase presented in Fig. 9). This context is considered for comparison as it is only achievable in the analog part of the receiver. We must not forget that at the output of the antenna we generally find a bandpass filter, see Fig. 4. Therefore, the ''RF/Matched filter'' filter presented at the receiver input should not be confused with the $H(f)$ filter which can be used in the digital part and on signals already filtered in a targeted frequency band and /or which are in baseband signals (BBS).

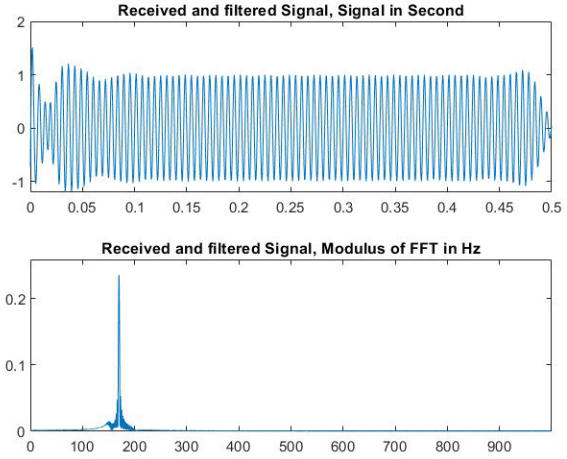

FIGURE 17. The observed and filtered signal, $x_f(t)$, and its spectrum $X_f(t)$.

Fig. 17 demonstrates that the filter was very effective since we can detect the target signal centered on the frequency 170Hz. It should be emphasized that in the temporal signal (i.e. the first image presented in this figure) undergoes atypical behavior at the beginning and at the end of the signal following the effect of the digital filtering carried out by $H(f)$.

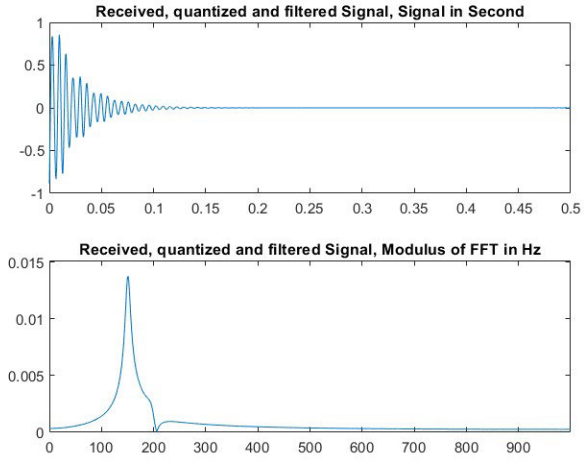

FIGURE 18. The quantized and filtered signal, $y_f[k]$, without the use of the non-linear function and its spectrum $Y_f[m]$.

In Fig. 18, we see that the signal filtered after passing through ADC no longer contains the target signal, which is completely lost. We can quickly see this by comparing this Fig. with Fig. 17. Indeed, the amplitude of the spectrum obtained, in Fig. 18, is about 15 times lower than that illustrated in Fig. 17. In addition, the spectrum in Fig. 18 is centered on the frequency 140Hz which could be a harmonic of the powerful interfering signal or a residual error (since the signal is annihilated).

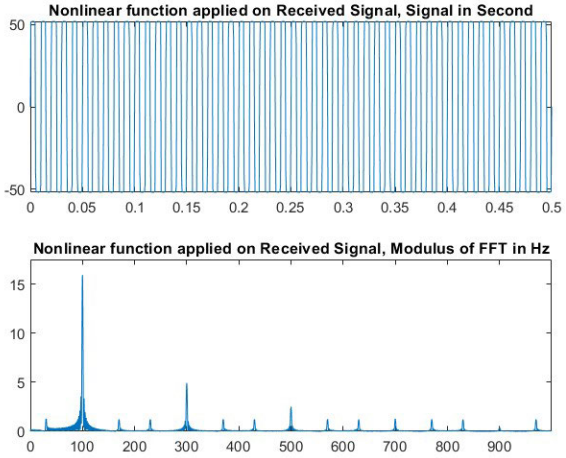

FIGURE 19. The signal after the non-linear function, $x_n(t)$, and its spectrum $X_n(f)$.

Equation (15) is selected as the nonlinear function $\Phi(x)$, with $\gamma = 50$. By comparing the results presented in Fig. 19 with those in Fig. 13, we can clearly see that the interfering signal has lost its power, and we also notice the different frequencies that appeared following the implementation of the non-linear function.

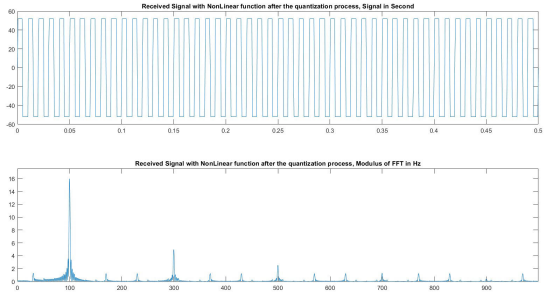

FIGURE 20. The quantized signal after the non-linear function, $y_n[k]$ and its spectrum $Y_n[m]$.

By comparing the results of two figures 20 and 15, we can highlight the interest of introducing the non-linear function; since in the last spectrum, we can see that the target signal has appeared, see the spectrum around 170Hz.

The results of the filtered signal after ADC clearly show that the non-linear function was able to protect the weak signal. Indeed, we see this by comparing the results presented in figures 18 and 21.

In Fig. 22, we see the interest of the non-linear function; in fact, this Fig. shows the difference between the spectra of the signal quantized and filtered with the non-linear function

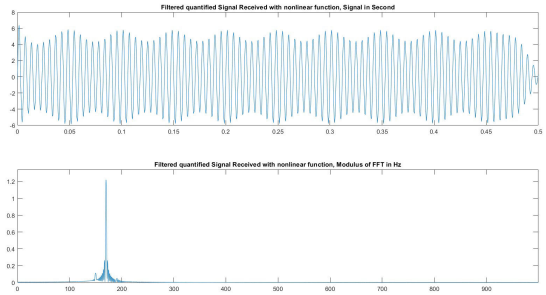

FIGURE 21. The spectrum of the quantized signal after the non-linear function, then filtered around the frequency $f = 170$Hz, $y_{fn}[k]$ and its spectrum $Y_{fn}[m]$.

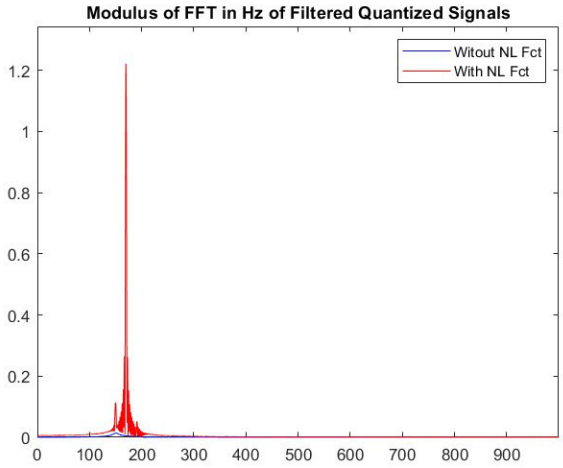

FIGURE 22. The spectrum of the quantized and filtered signal with and without a non-linear function, $Y_f[m]$ and $Y_{fn}[m]$.

$Y_f[m]$ and of the signal quantized and filtered without non-linear function $Y_{fn}[m]$.

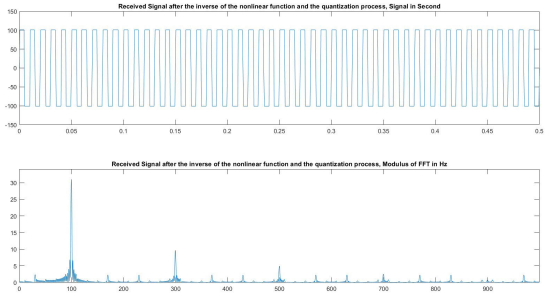

FIGURE 23. The signal after the inverse non-linear function, $x_{in}[k]$ and its spectrum $X_{in}[m]$.

In Fig. 23, we have applied the non-linear inverse function in the digital part of the receiver. The last step in our reception chain then consists of filtering the signal $x_{fin}[k]$ by the filter $H(f)$. In Fig. 24, the target signal was well obtained but with a residual non-linear effect.

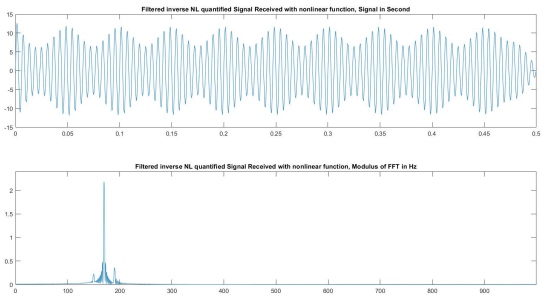

FIGURE 24. The signal at the output of the processing chain, $x_{fin}[k]$ and its spectrum $X_{fin}[m]$.

C. OFDM SIGNALS

By carrying out several simulations on simple periodic signals or the sum of periodic signals; we observed encouraging results as it was observed in the simulation presented in the previous subsection. Two types of broadband signals can be considered in our study, [22]:

- Ultra-wideband communications, UWB which are carried out using short pulses, less than a nano-second and which extend over a very wide frequency spectrum, [23].
- Orthogonal Frequency Division Multiplexing (ODFM) which is a very important modulation for high speed and broadband communication systems like (Wireless Personnel Area Network (WPAN), Wireless Fidelity (WiFi), etc), [24].

As the nature of the processed signals has little effect on the results of our study, we chose to carry out our simulations using only broadband signals of type OFDM, [25]. Orthogonal Frequency Division Multiplexing (OFDM) is a form of modulation that divides a high data rate across many narrow-band subcarriers to protect against frequency-selective fading. OFDM has been adopted by the WiFi standard and widely used in communication standards (WiFi, Enhanced WiFi, Lightbridge, OcuSync, etc.) for drones. It has also been chosen for LTE and LTE-A cellular telecommunications, whose commercial name is 4G. OFDM has also been used in many wireless broadband systems thanks to its many advantages. One of the main advantages of OFDM is concerning its resistant to frequency selective fading. OFDM also allows efficient use of available spectrum, see Fig. 25, and is resistant to InterSymbol Interference (ISI).

To highlight the vicinity issue between two OFDMs, we created an OFDM modulation of 32 orthogonal subcarriers, in the 900 MHz band. Each subcarrier carries a signal modulated in Quadrature Phase Shift Keying (QPSK), and has a spectral bandwidth of 500 kHz (corresponding to a symbol time $Ts = 2$ ms). Each OFDM signal occupies a 16MHz band. The choice of the parameters depends on the performance of the system. For example, a high data rate requires a short symbol time. Good tolerance on propagation delay results in a large number of carriers and a small space between subcarriers. However, good tolerance to Doppler

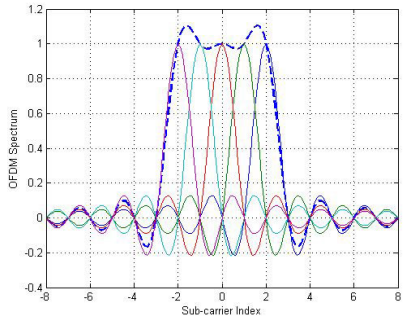

FIGURE 25. The spectrum of a simple OFDM signal with a reduced number of carriers to illustrate the concept of this type of signal.

effects requires a reduced number of carriers and a large space between subcarriers. Hereinafter, the useful signal is centered on 928 MHz while the jamming signal is centered on 908 MHz. Then, it remains to superimpose the two signals in accordance with the dynamic range of 80 dB, see Fig. 26.

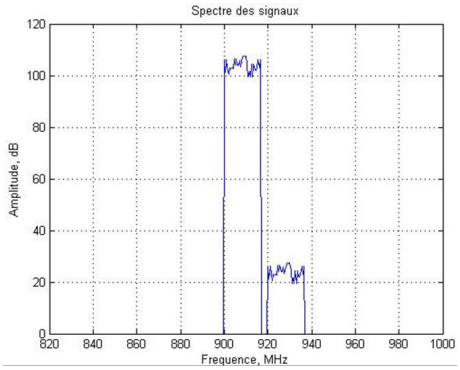

FIGURE 26. The spectrum of the received signal: the sum of the two OFDMs with a high amplitude ratio.

To test the impact of a non-linear receiver on OFDM broadband signals, we considered the case illustrated by Fig. 27, where the observed signal is generated according to the following model:

$$x(t) = \alpha s(t) + \beta i(t) + n(t) \tag{15}$$

with $s(t)$ is the signal of interest.

With a frequency band B_S, the interference is given by $i(t)$ with a frequency band given by B_I, we also consider that $E\{s(t)\} = E\{i(t))\} = 0$ and $E\left\{s^2(t)\right\} = E\left\{i^2(t)\right\} = 1$, the frequency bands of the two signals $s(t)$ and $i(t)$ are separated by:

$$\delta f = \Delta f - \frac{B_I + B_S}{2} \tag{16}$$

with Δf the difference between the two central frequencies of $s(t)$ and $i(t)$. We also assume that the amplitude gains of the two signals are $\beta \gg \alpha$, see Fig. 27. We then carried out several simulations with different parameters.

In this section, we use the signals shown in Fig. 9 and consider the model presented in equation (15), with:

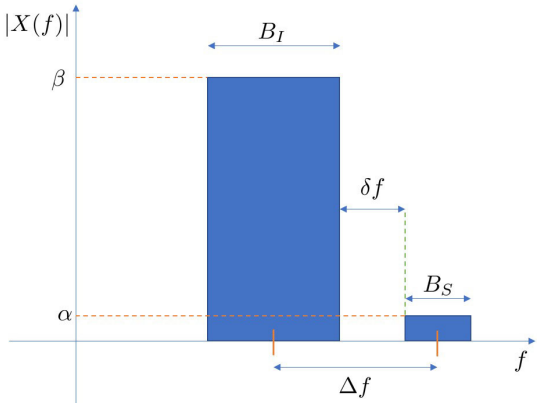

FIGURE 27. A generic scenario with two OFDM signals as by the model $x(t) = \alpha s(t) + \beta i(t) + n(t)$.

- The observation duration was almost 4.7 ms which corresponds to a vector of $7 * 10^4$ samples,
- The interfering signal $i(t)$ is another OFDM signal, with $N_{ISub} = 32$ subcarriers, the symbol duration $T_{ISym} = 0.1$ms, the carrier frequency was chosen $f_{IC} = 1.3\ MHz > \frac{4N_{ISub}}{T_{ISym}} = 1.28$MHz, the cyclic prefix was 5%, the binary sequence was modulated in QPSK, the frequency band of the signal was $B_I = 320$kHz.
- The signal of interest $s(t)$ is also an OFDM signal, with $N_{SSub} = 16$ subcarriers, the symbol duration $T_{SSym} = 0.1$ms, the frequency of the carrier was chosen $f_{IS} = 1.9\text{MHz} > \frac{4N_{SSub}}{T_{SSym}} = 640$kHz, the cyclic prefix was 6%, the binary sequence was modulated in Binary Phase Shift Keying (BPSK), the frequency band of the signal was $B_S = 160$kHz.
- The difference between the two central frequencies is $\Delta f = 600$kHz and the space between the two frequency bands is given by $\delta f = 360$kHz.
- $\alpha = 1$ and $\beta = 100$ to have a ratio of 40dB between the two signals, so the signal of interest is completely hidden by the jammer signal $i(t)$.

Fig. 28 shows a weak target signal $s(t)$.

The sampling frequency f_s should satisfy the following constraints:

$$f_s > \max\left(2f_{Ic} + \frac{N_{ISub}}{T_{ISym}}; 2f_{Sc} + \frac{N_{SSub}}{T_{SSym}}\right) \tag{17}$$

To clearly illustre the importance of various parameters (such as the effect of quantization, sampling, non-linear function etc.), we fixed the sampling frequency in this simulation at the value $f_s = 15$MHz, well above the threshold fixed by the Nyquist sampling theorem. To accentuate the quantization problem, we can select $N \approx 6$. However, to better illustrate the effects, we decided to minimize $N = 2$ as much as possible so that the interfering signal keeps its characteristics and the target signal almost disappears at the analog-to-digital converter output. In Fig. 29, we can notice that the weak signal has almost disappeared; and we also see

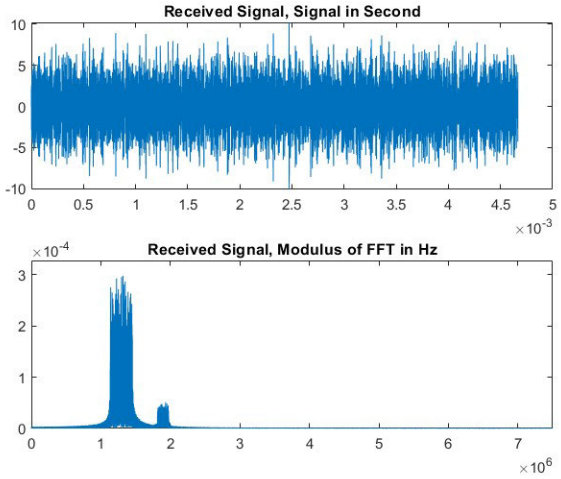

FIGURE 28. The observed signal $x(t)$ and its spectrum $X(f)$.

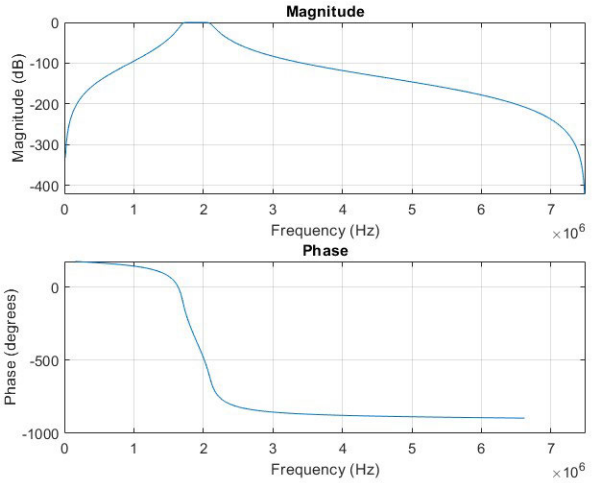

FIGURE 30. The amplitude and phase of the bandpass filter, $H(f)$, centered on the spectrum of the useful signal.

the harmonics of the main signal which are much stronger than the target signal.

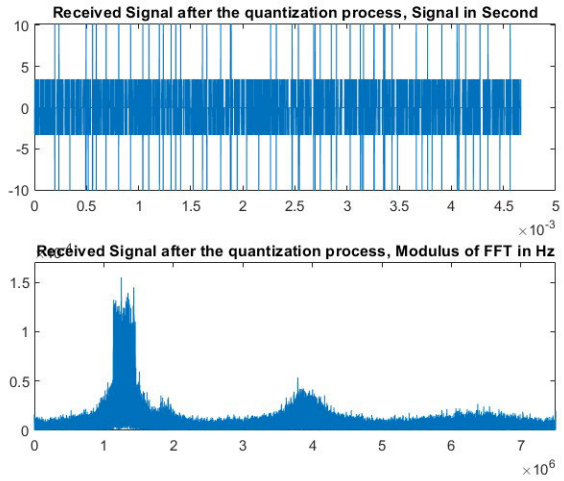

FIGURE 29. Te quantized signal $y[k]$ and the corresponding spectrum $Y[m]$.

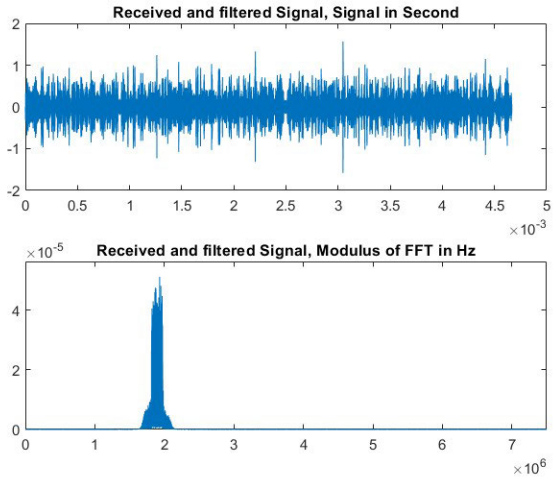

FIGURE 31. The observed and filtered signal, $x_f(t)$ with $X_f(t)$.

To recover the target signal $s(t)$, we implemented a ''Butterworth'' bandpass filter, of order 6, with its cutoff frequencies $f_{c1} = 1.7$MHz and $f_{c2} = 2.1$MHz,

To show the effectiveness of the filter, we applied this filter, $H(f)$, on the received signal $x(t)$ in an ideal context (i.e. the ''ideal situation'' phase presented in the Fig. 9). Fig. 31 demonstrates that the filter was very effective since we found the target signal centered on the frequency 1.9MHz.

In Fig. 32, we see that the spectrum of the filtered signal after passing through the ADC has been strongly affected. We can quickly see this by comparing this figure with Fig. 31.

The nonlinear function $\Phi(x)$, is selected according to equation (15) with $\gamma = 15$. By comparing the results presented in Fig. 33 with those in Fig. 28, we can notice the different frequencies that appeared following the introduction and choice of the non-linear function.

By comparing the results of two figures 34 and 29, we also see the interest of introducing the non-linear function; as the SINR has been improved.

The results of the filtered signal after ADC clearly show that the non-linear function was able to protect the weak signal. Indeed, we see this by comparing the results presented in figures 32 and 35.

In Fig. 36, we see the interest of the non-linear function; in fact, this figure shows the difference between the spectra of the quantized and filtered signal with the non-linear function $Y_f[m]$ and of the quantized and filtered signal without the use of the non-linear function, $Y_{fn}[m]$.

In Fig. 37, we have applied the inverse non-linear function in the digital part of the receiver. The last step in our reception chain then consists of filtering the signal $x_{fin}[k]$ by the filter

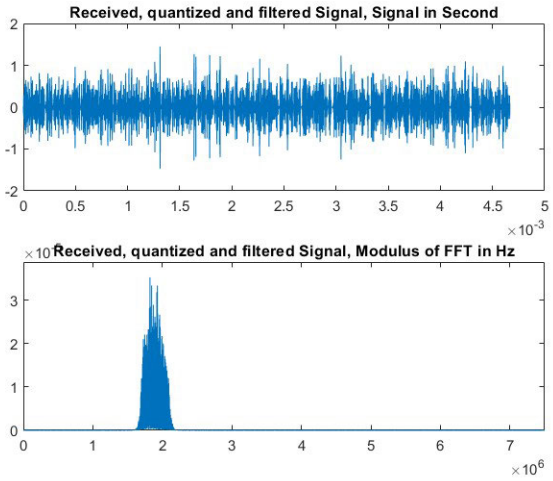

FIGURE 32. The quantized and filtered signal, $y_f[k]$, without the use of the non-linear function and its spectrum $Y_f[m]$.

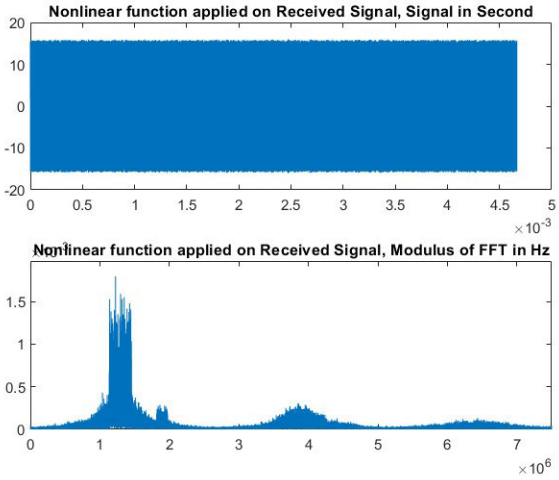

FIGURE 33. The output of the non-linear function, $x_n(t)$, and its Fourier transform $X_n(f)$.

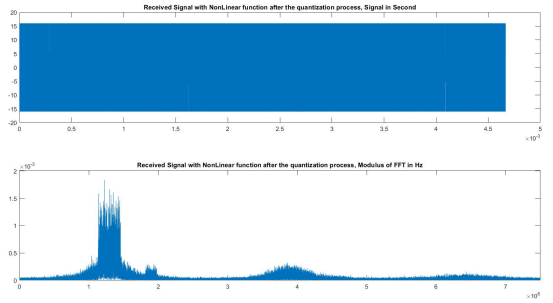

FIGURE 34. The quantized signal after the non-linear function, $y_n[k]$ and its spectrum $Y_n[m]$.

$H(f)$. Fig. 38 shows that the target signal was well obtained but with a residual non-linear effect.

V. NON-LINEAR CIRCUITS

In certain situations, we need to receive signals with great dynamics: one very powerful emission and another could

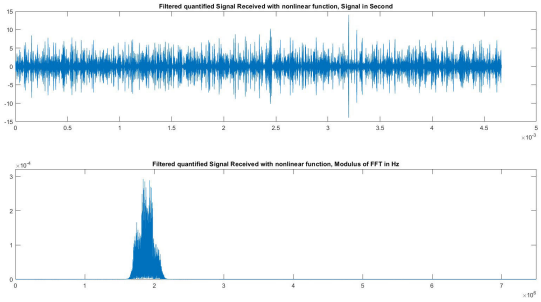

FIGURE 35. The spectrum of the quantized signal after the non-linear function, then filtered around the frequency $f = 170Hz$, $y_{fn}[k]$ and its spectrum $Y_{fn}[m]$.

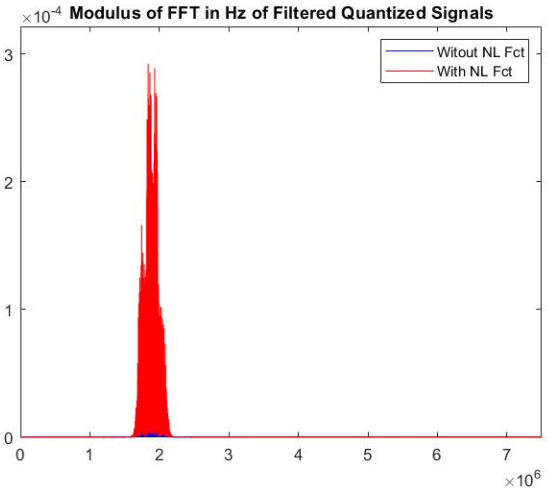

FIGURE 36. The spectrum of the quantized and filtered signal with and without the non-linear function, $Y_f[m]$ and $Y_{fn}[m]$.

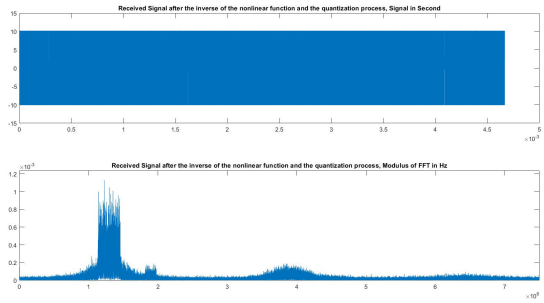

FIGURE 37. The signal after the inverse non-linear function, $x_{in}[k]$ and its spectrum $X_{in}[m]$.

be a very weak one. In this case the extraction of the weak signal becomes very difficult, especially in a non-cooperative context. One possibility is to compress the signal amplitudes, to avoid the use of a sophisticated, energy-demanding and expensive ADC with a large number of bits [26], [27]. After reducing the dynamics of the signals, we can convert our signals to digital using a normal ADC.

In previous sections, we approached the problem and discussed the contribution of our proposed solution which consists of introducing into the reception chain a bijective

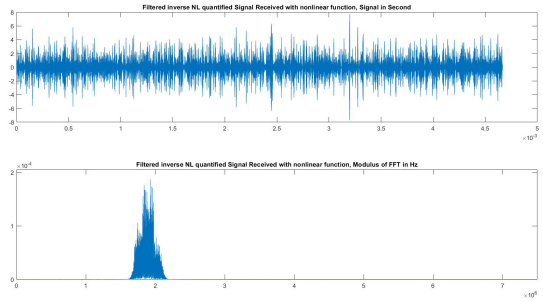

FIGURE 38. The output of the reception chain, $x_{fin}[k]$ and its spectrum $X_{fin}[m]$.

non-linear function and its inverse. We have seen the importance of the choice of this function and the effect of the parameters on the obtained results. The important questions become: as the non-linear function had to be introduced in the analog part of a reception chain and its inverse in the digital part, then can we realize this function using analog electronic circuits? If so, how and what are its characteristics?

The goal of this part of our research project is to develop and test different analog systems in order to reduce the dynamics of the signals to better separate them. Subsequently, it was necessary to evaluate the performance of the systems thus simulated according to their non-linear transfer functions and their bandwidths. We have tried to improve the bandwidth for each circuit. The simulated signals occupy large, adjacent spectral bands.

Concerning the reduction of the dynamic range of signals, we have discussed in previous sections the need to introduce a non-linear function in the analog part of our processing chain and another digital function which plays the role of the inverse function. In the literature, several non-linear circuits are proposed. Mathematically speaking, we can designate an infinite number of non-linear functions, a large majority of these functions can be approximately implemented in electronic circuits. On the other hand, the function that interests us must have several properties:

- This function must be achievable using a simple circuit (to reduce energy consumption and price and simplify the manufacturing steps).
- The transfer function of the selected circuit must best approximate the desired function.
- The simulated circuit must have a wide bandwidth.
- The inverse function exists and is feasible digitally.

Hereinafter, we analyze several circuits capable of satisfying the above conditions.

A. LOGARITHMIC AMPLIFIERS

In certain situations, receivers may be interfered by high-power interference sources. Thus, the received signal can be considered as the sum of a strong interfering signal and the weaker target signal. Even if the two signals do not overlap in the frequency domain, it will be difficult to process the useful signal, as it might disappear at the output of the analog-to-digital converter (ADC). Indeed, the majority of modern transmission systems are digital requiring sampling and quantization of analog signals received by the receiver.

The transition from analog to digital requires the use of an ADC with a limited number of quantization bits. If the power ratio between the two mixing signals is too high, the weak signal can be lost at the ADC output, [28]. To avoid such scenario, it is possible to introduce a non-linear module into the reception chain in order to reduce the power difference between the two signals. By placing an analog circuit before ADC that compresses the amplitude, it is possible to reduce the resolution of ADC [29]. The mathematical function chosen will be very close to a logarithmic function. Indeed, this type of function has the property of compressing the strong signal without modifying the weak signal. Furthermore, the logarithmic function is invertible. This last property is important, if we expect to recover the information contained in the signal. Applications of this technology could improve the performance of radio communication receivers. Indeed, electronic warfare systems are faced with a significant dynamic range which limits their analysis capabilities.

1) POSSIBLE RESPONSES FOR LOGARITHMIC AMPLIFIERS

The ADC commonly used in digital radio communication receivers has 12 to 16 bits. To cover a high dynamic range with a reasonable number of bits, we can introduce a logarithmic amplifier as a nonlinear unit before the ADC. The Logarithmic Amplifier outputs a voltage that varies linearly with the logarithm of the input. Low amplitudes are more amplified than large amplitudes. Thus, an amplitude compression is carried out, which is a non-linear operation. After digital conversion, the signals must be decompressed by the inverse mathematical function to be able to process data.

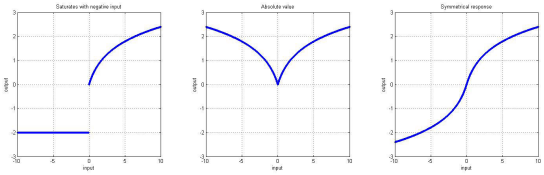

FIGURE 39. Different possible answers for a logarithmic amplifier: amplifier with saturation for a negative input, Absolute value amplifier and symmetrical amplifier.

Symmetrical logarithmic amplifiers are the best suitable to our application, since they are easily invertable in the digital part of our processing chain. According to [30], there are two types of logarithmic amplifier: true and demodulation types. True logarithmic amplifiers provide the logarithm of the signal without demodulating the signal. In contrast, demodulating logarithmic amplifiers provide the logarithm of the signal envelope. Logarithmic demodulators and amplifiers are widely used in radars and some radio receivers.

2) LOGARITHMIC FUNCTION WITH A DERIVATIVE CIRCUIT

The logarithmic function can be achieved using several circuits. As an example, we can implement a logarithmic function of a signal, $x(t)$, by using a circuit consists of two stages in parallel (a derivative $\frac{\partial}{\partial t}$, and an inverse $\frac{1}{x(t)}$) followed by two other circuits and in cascade (a multiplier and an integral circuit), i.e.:

$$\ln(x) = \int_0^t \frac{1}{x(\tau)} \frac{\partial x(\tau)}{\partial \tau} d\tau$$

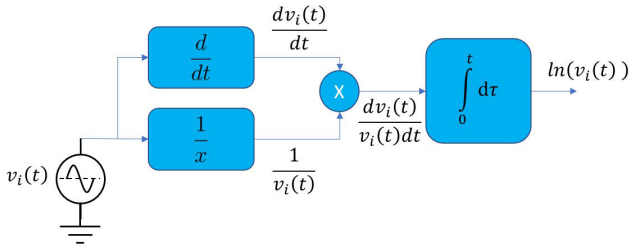

FIGURE 40. A concept of a logarithm amplifier.

The major disadvantage of such a circuit, shown in Fig. 40, is the use of the derivative system which is difficult to achieve in practice. Indeed, it should be noted that the main components used in this circuit (the differentiator, the inverter, the multiplier and the integral) are largely introduced in control, robotics, or to a certain limit in telecommunications. On the other hand, the electrical circuits to carry out these functions (especially, the differentiator or the inverter) are not perfect and they suffer from several limitations linked to their approximation errors, their bandwidths and certain undesirable non-linear effects. In practice, the implementation of such circuits can't be used in a wide-band and wide-dynamic logarithmic function. For these reasons, this circuit was not considered in our simulations.

3) TRUE LOGARITHM AMPLIFIER

In some applications like radio receivers, an Automatic Gain Control (AGC) circuit can be used to reduce the dynamic range of the output. In other applications, such as radar receivers, the settling time of the AGC cannot be tolerated. As part of the design of a tracking radar (Moving Target Indication Radar, MTIRadar), the authors of [31] presented a circuit able of making a "True Logarithmic Amplifier" with a Phase Matching of the order of 14° with a large amplitude dynamic of 80dB around the frequency 70MHz. In radar, phase information is important since the amplifier output must be centered on the intermediate frequency (IF). A logarithmic amplifier can assist the system in separating a target signal from an unwanted one, such as clutter signals caused by raindrops.

To explain the idea of the "True Logarithmic Amplifier", we first present a basic cell, see Fig. 41. This figure shows a basic cell of the True Logarithmic Amplifier and its transfer function of the amplifier "A" with its saturation limit. According to that figure, we can show that:

$$V_{out} = \begin{cases} (1+A)V_{in} & \text{If } |V_{in}| \leq V_{IL} \\ (V_{OL} + |V_{in}|)\,\text{Sgn}(V_{in}) & \text{Ifnot} \end{cases} \quad (18)$$

with "Sgn" stands for the sign function, A is the gain of the amplifier, V_{IL} and V_{OL} are the input and output limits of the amplifier A with its saturation limit. Then, we can see that $V_{IL} = V_{OL}/A$; to simplify our notation, we note hereinafter V_{OL} by V_L.

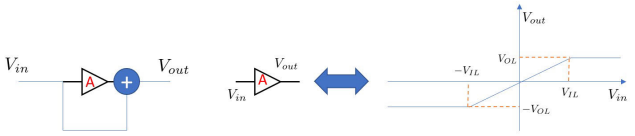

FIGURE 41. At left: a basic cell of the True Logarithmic Amplifier, Input Voltage: V_{in}, Output Voltage V_{out}. Right: the transfer function of a linear amplifier with a saturation limit.

The input of a cell follows equation (18), until the mth cell where a saturation is reached at the output, so $V_{om} = V_L(1 + \frac{1}{A})$. If the total number of cells is N, then the signal passes through $N - m$ cells with saturation. The final output of N cell therefore becomes:

$$\begin{aligned} V_O &= (N-m)V_L + V_L\left(1 + \frac{1}{A}\right) \\ &= V_L\left(N + \frac{1}{A} + 1 - m\right) \end{aligned}$$

The input signal is linearly amplified by $m-1$ cells before reaching the saturation:

$$\frac{V_L}{A} = V_{in}(1+A)^{m-1} \quad (19)$$

We can then estimated the value of m:

$$m = 1 + \left\lceil \frac{\log\left(\frac{V_L}{AV_{in}}\right)}{\log(1+A)} \right\rceil \quad (20)$$

where the upper integer part is defined by $n = \lceil x \rceil \in \mathbb{N}$ and $n \geq x$. So, the final output of the True Logarithmic Amplifier with N cells becomes:

$$V_O = \left(N + \frac{1}{A} + \left\lceil \frac{\log\left(\frac{AV_{in}}{V_L}\right)}{\log(1+A)} \right\rceil\right) V_L \quad (21)$$

It has been shown that with a relatively large N, the output of the True Logarithmic Amplifier is able to approximate a logarithmic function. As this type of amplification is widely answered in the literature, we chose to study the logarithmic amplifier including cascaded amplifiers. The principle of this architecture is to place amplification circuits in a chain. The idea is this: a high amplitude signal can saturate the first amplifier. Then, it will go through all the stages in a saturation state. For a weak signal, the behavior is different: the signal is amplified linearly by the first stage, then by the other stages. If the signal is quite weak, it can pass through all the steps

without reaching saturation. The gain of the chain is the sum of the gains (dB) of each stage. Each stage is a non-inverting amplifier. The gain is determined by:

$$V_s = V_e \frac{R_g}{R_g + R_f} \quad G = \frac{R_g + R_f}{R_g} \tag{22}$$

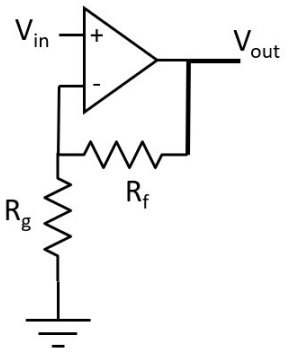

FIGURE 42. Non-Inverting Amplifier.

This type of circuit tolerates a negative input. We can notice that the transfer function is not invertible when the signal reaches the saturation state. It is therefore necessary to ensure that the amplitude of the useful signal does not cross a certain threshold value.

In the circuit shown in Fig. 43, we have only simulated a circuit with three amplifiers to show the concept. In the literature, a true logarithmic amplifier should consist of above six stages, each with 10 dB of gain.

According to Fig. 44, the gain is linear. This system does not make it possible to obtain a good logarithmic amplifier. Indeed, this circuit can saturate high amplitude signals. Signals reaching the saturation state are lost in the reception chain. The propagation delays of the different stages must be studied carefully if we choose this type of circuit. For a wideband signal, the phase shift can deteriorate the signal. The impulse response of the circuit is illustrated in Fig. 52. In the last figure, we observe a bandwidth of almost 5MHz.

In Fig. 53, we observe the saturation effect for a simple sinusoidal input signal with a frequency of 1 MHz.

4) DIODE-BASED LOGARITHMIC AMPLIFIERS

The simplest circuit for making a logarithmic amplifier is based on an operational amplifier looped by a nonlinear dipole, which can be a diode. These circuits are mainly used for compression range: if the amplitude of the input signal varies from a few times to a few dozen times. This type of signal can normally saturate a linear amplifier, but not a logarithmic amplifier [32].

Logarithmic converters are based on an amplifier with a PN junction or MOSFET transistor in a feedback loop. These converters provide excellent logarithmic response in low frequency applications. To build a logarithmic amplifier, we can use the exponential variation of the current, $i(t)$ measured in Amperes, as a function of the voltage, $v(t)$ measured in Volts, in a diode:

$$i(t) = I_S \left(\exp\left(\frac{v(t)}{\eta V_T} \right) - 1 \right) \approx I_s \exp\left(\frac{V}{\eta V_T} \right) \tag{23}$$

with the saturation current[6] I_s is measured in A, the emission coefficient $1 \leq \eta \leq 2$ depends on the nature of the semiconductor ($\eta = 1$ for Germanium and $\eta = 1.3$ for silicon), the thermal voltage $V_T = \frac{kT}{q}$ measured in Volts, Boltzmann's constant $k = 1.38 * 10^{-23}$ in Joules/degree Kelvin, T the temperature in Kelvin, $q = 1.6 * 10^{-19}$ Coulomb. So at an ambient temperature of $20°C$, $T = 293°K$ and $V_T \approx \frac{1}{40} V$, therefore for $\forall v(t) > 0$ then $i(t) \approx I_s e^{40v(t)}$. Based on equation (23), we can find that:

$$v(t) = \left(\frac{\eta k T}{q} \right) \ln\left(\frac{i(t)}{I_s} + 1 \right) \tag{24}$$

An ideal amplifier is characterized by two equations, see Fig. 47:

$$I_+ = I_- = 0 \quad V_+ = V_- \tag{25}$$

where I_+ and I_- (resp. V_+ and V_-) are the currents (resp. voltages) at the nodes $(+)$ and $(-)$ of the amplifier. Using equations (23) and (25) and based on the circuit proposed in Fig. 47, we can deduce the following equations:

$$I_+ = I_- = 0 \Rightarrow I_R = I_D = I \tag{26a}$$

$$V_+ = V_- = 0 \Rightarrow V_{in} = IR \quad \& \quad V_{out} = -V_D \tag{26b}$$

By substituting the current of the diode I by its value given by equation (23) in equation (26b), we deduce that the transfer function of the logarithmic amplifier is given by:

$$I \approx I_s \exp\left(\frac{V_D}{\eta V_T} \right) \Rightarrow V_D = \eta V_T \ln\left(\frac{I}{I_S} \right)$$

$$\Rightarrow V_{out} = -\eta V_T \ln\left(\frac{I}{I_S} \right) = -\eta V_T \ln\left(\frac{V_{in}}{R I_S} \right)$$

This type of circuit performs a logarithmic conversion just for positive inputs, but it saturates when the input becomes negative, see Fig. 49. This behavior requires the use of an a positive voltage offset with the input signal.

Furthermore, the frequency response shows us that this circuit behaves like a low-pass filter, see Fig. 50. Pspice offers several models of operational amplifiers. Each has its own characteristics and frequency limitations. The LF411 used in the simulation cannot exceed 100 kHz. This architecture does not meet the needs of our project. The need to use a unipolar signal is not satisfactory. Yet this circuit establishes a reference point for other proposals.

Fig. 51 shows the effect of non-linearity on a simple signal.

[6]The saturation current, or reverse current, depends on the width of the semiconductor, diffusion coefficients, doping concentrations, and other intrinsic parameters of the diode. It can vary from few femto to around ten micro Amperes, $I_S \in \left[10^{-15}, 10^{-4}\right] A$.

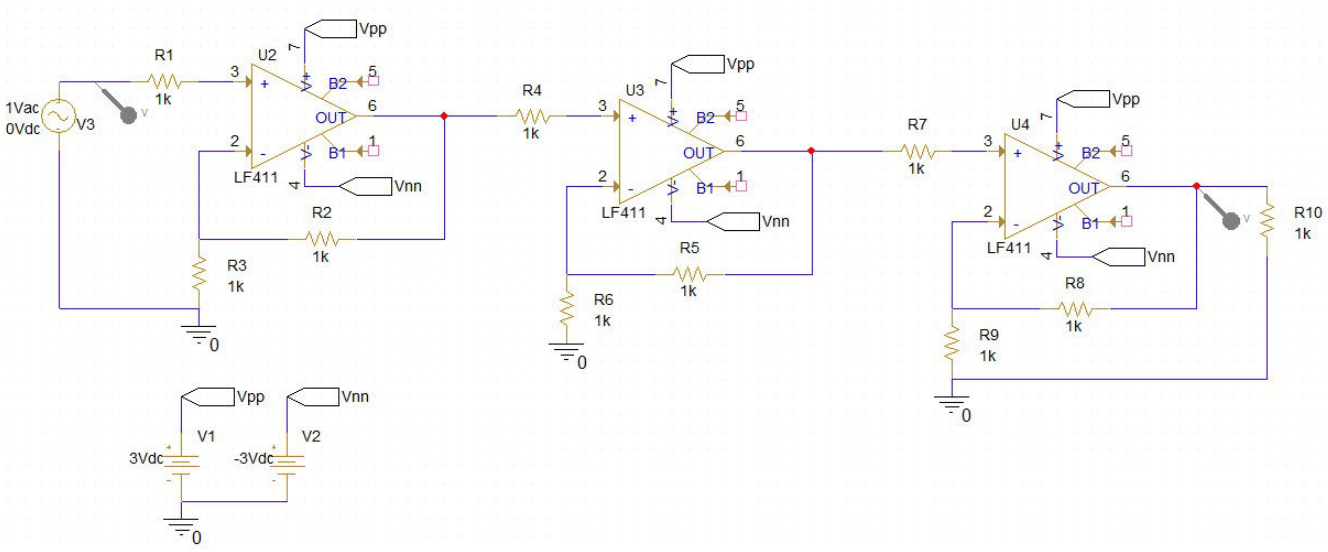

FIGURE 43. Simulation of a cascaded amplifier.

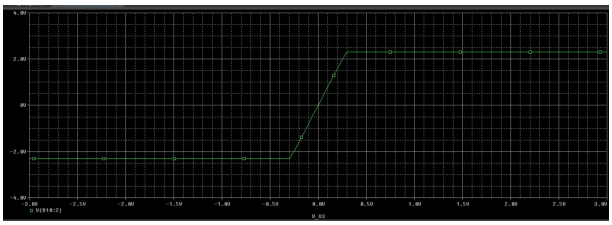

FIGURE 44. The output-input relationship of a cascaded amplifier.

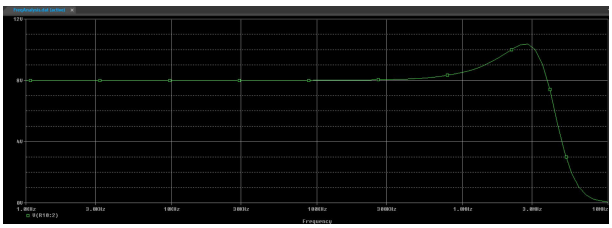

FIGURE 45. The transfert function of a cascaded amplifier.

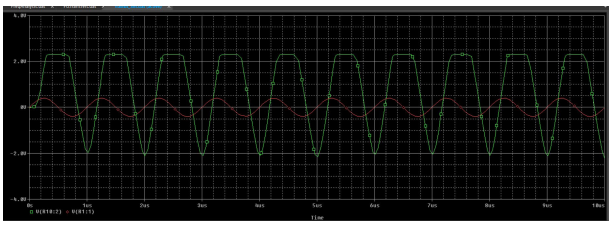

FIGURE 46. The saturation effect with a simple input signal.

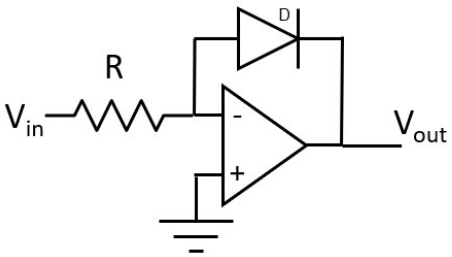

FIGURE 47. A logarithmic amplifier with a diode feedback.

5) DUAL GAIN STAGE

The logarithmic amplifier commonly used for signal processing is called the true logarithmic amplifier introduced in [33]. The main idea is to realize the logarithmic amplifier by cascading circuits using two amplifiers in parallel with different gains. Each cell contains two independent amplifiers having the same input: one amplifier with high gain and low saturation level, the other with unity gain and high saturation level. This dispositive is equivalent to an elementary amplifier with a sharp change in gain at the saturation level of the first amplifier. A true logarithmic amplifier should consist of six ideal double-gain stages, each with 10 dB of gain.

To improve the basic structure presented in the previous paragraph, we replaced each stage with a double-stage gain. Each stage contains two independent amplifiers with a common input. In theory, the transfer function becomes logarithmic instead of linear.

Fig. 52 represents a double gain stage. There are two inverting amplifiers, one with a unity gain, and the other with a higher gain. Then, an amplifier sums the two amplified signals. Fig. 53 shows the function between the input and output of the circuit.

The non-linear effects of the circuit can be seen in Fig. 54.

The bandwidth of the circuit is limited by the band of the chosen operational amplifier. In this simulation, we select the LF411 to present the principle, see Fig. 55. The LF411 has a bandwidth limited to 500KHz.

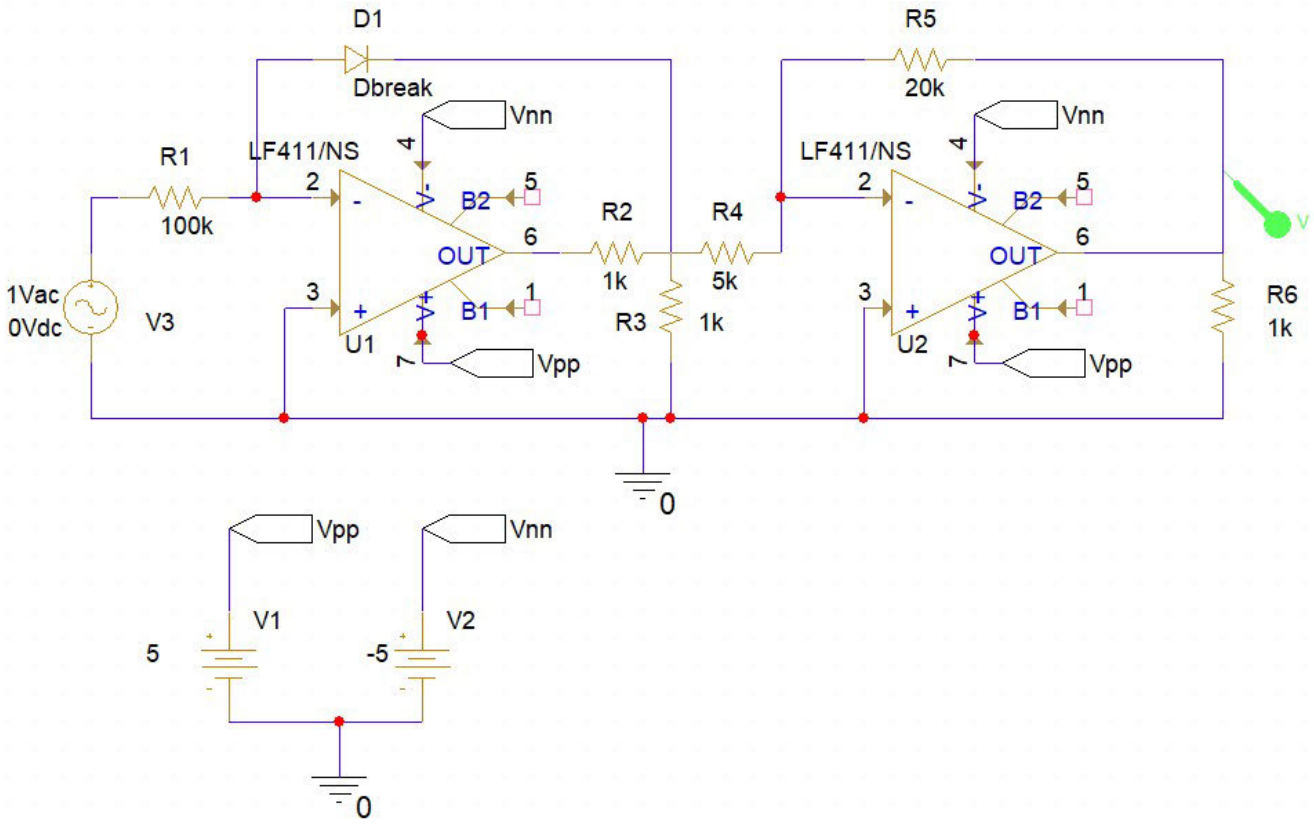

FIGURE 48. The logarithmic amplifier with a diode.

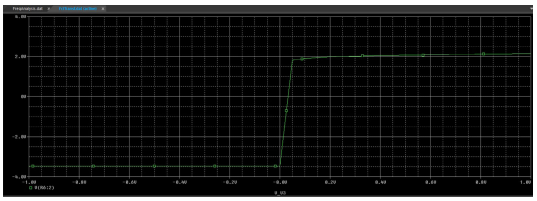

FIGURE 49. Input-Output relationship of the logaritmic amplifier.

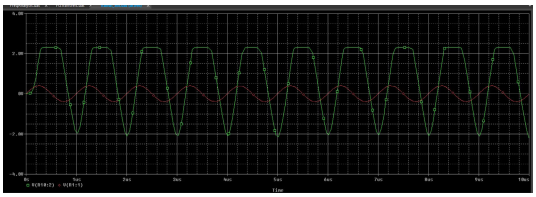

FIGURE 51. Nonlinear effects of the logarithmic amplifier with a diode.

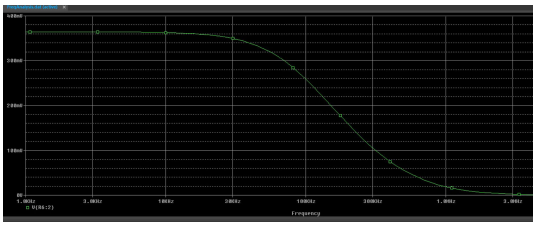

FIGURE 50. The frequency transfer function of the logarithmic amplifier with a diode.

6) SYMMETRICAL AMPLIFIER

The voltage across a diode is proportional to the logarithm of its current. To exploit this property, we introduced a differential amplifier based on an operational amplifier. A non-inverting amplifier can be placed at the output. The circuit thus proposed performs a non-linear function. To handel negative values, we used a voltage rectifier including two diodes. Then, we placed an input voltage follower circuit used as a buffer amplifier to eliminate loading effects. A new circuit is presented in Fig. 56.

The transfer function of this circuit has needed properties, see Fig. 57. Indeed, it is symmetric for negative values and performs logarithmic conversion. Amplifier gain is used to adjust the amplification of weak signals. The frequency response is higher than that obtained for previous circuits, although the circuit still behaves like a low-pass filter, see Fig. 58.

A wide range of commercially available wide-band operational amplifiers can be found. The circuit proposed in this paragraph can be considered with other components, as an example, we cite two other types of amplifier available:

B. SQUARE ROOT CIRCUIT

The square root function can be considered as another candidate for our application, [34]. The root of a number can

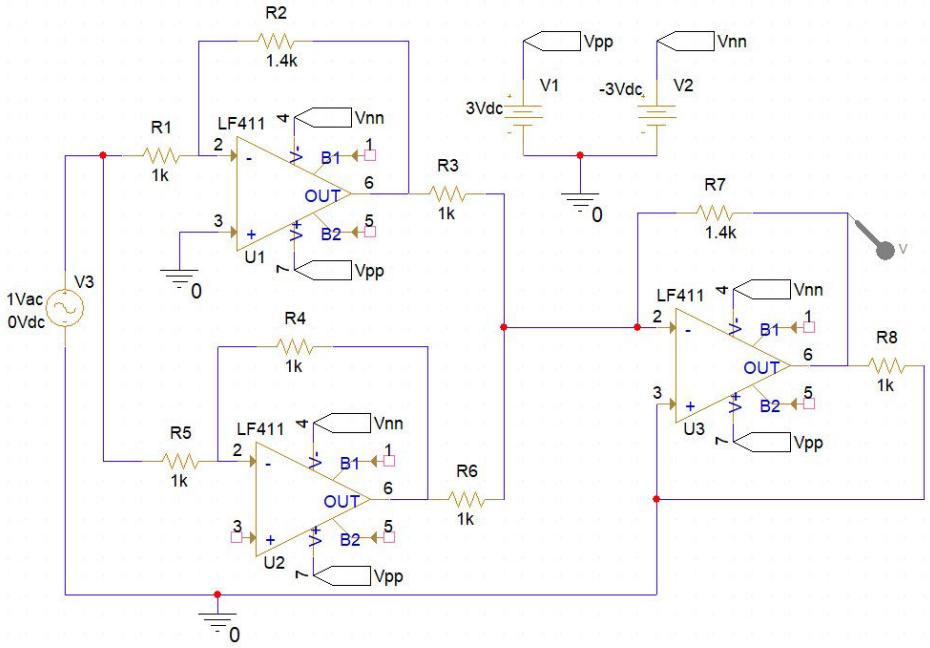

FIGURE 52. Simulation of an amplifier with a Dual Stage Gain.

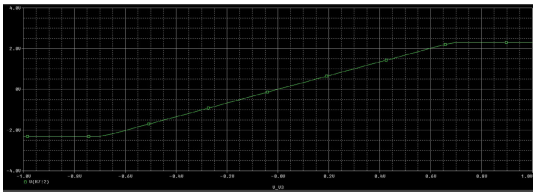

FIGURE 53. Input - Output relationship of an amplifier with Dual Stage Gain.

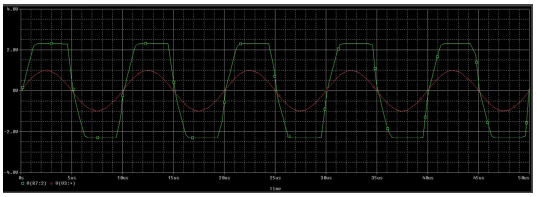

FIGURE 54. Non-linear effects of a Dual Stage Gain amplifier.

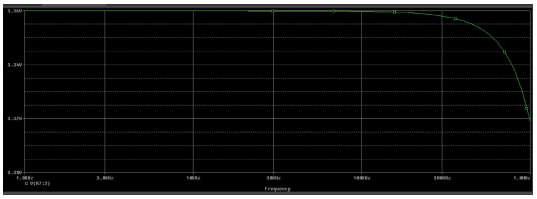

FIGURE 55. Simulation of a Symmetrical Amplifier.

be obtained by multiplying its log by $\frac{1}{2}$, and then taking the anti log. A possible circuit for the square root was presented in [35]. In their proposed circuit, an operational amplifier, called "A1", and a transistor "Q1" form the logarithmic converter for the input signal. The output of this converter

TABLE 1. The characteristics of two potential operational amplifiers.

	Analog Device	Texas Instrument
Composante	AD8615AUJ	LMH6624MF/NOPB
Bandwidth	24 MHz	1.5 GHz
Slew Rate	12 V/μs	400 V/μs

feeds another transistor "Q2" which produces a level shift for the voltage of the divider controlled by the ratio of two resistors $\frac{R_4}{R_5}$. The divider thus reduces the logarithmic voltage by a factor depending on the theoretical root and the excitation of a buffer amplifier "A2". The level shift transistor, "Q3", used in diode equivalent mode of operation. The feedback from "A2" ensures the necessary voltage at the circuit output. Two other transistors "Q2" and "Q3" are connected in diode mode. Finally, a gain resistor, "R7", has been introduced to maintain the currents in "Q2" and "Q3" relative to the variations in the signal levels [35]. We simulated a simplified version of the proposed circuit using Pspice: by eliminating certain components which control saturation of the current and voltage, see Fig. 60. Because, the omitted components do not affect bandwidth or the input-output relationship.

Our simulations show the saturation function illustrated in Fig. 61, which is similar to the true square root function, is asymmetric, so it cannot be used for zero-mean signals. To handel the last problem, we can introduce a direct current source in series with the input signal. The voltage of the DC source V_S must be well chosen so that the sum of this voltage with the input signal no longer reaches a negative value. In this case, the circuit is characterized by an asymmetric function: almost linear when the input signal

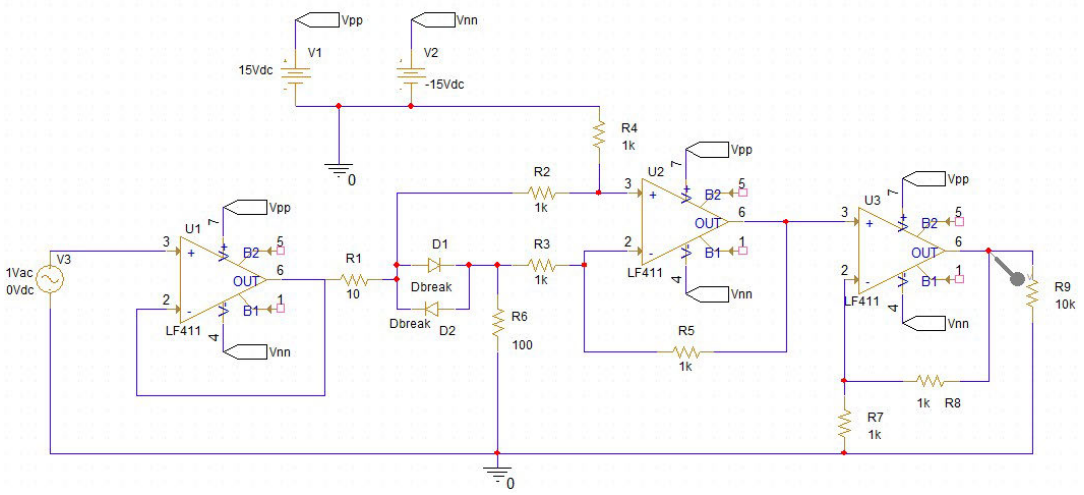

FIGURE 56. Simulation of an amplifier with a Dual Stage Gain.

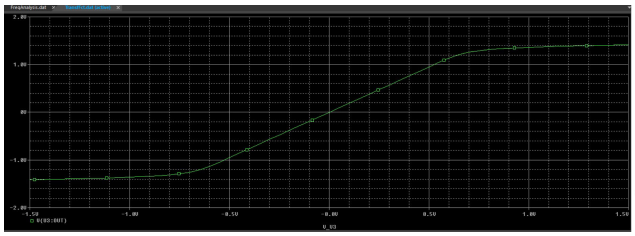

FIGURE 57. The transfer function of a symmetrical amplifier.

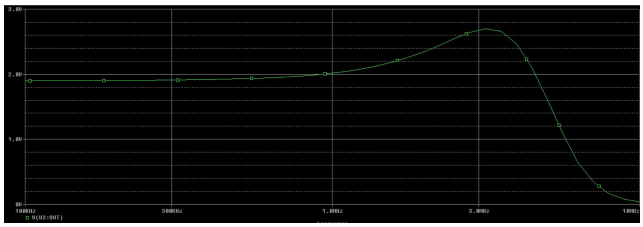

FIGURE 58. The frequency response of the symmetrical amplifier.

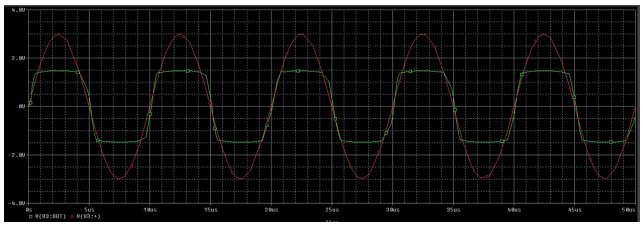

FIGURE 59. The nonlinear effect of a symmetrical amplifier.

shows a negative voltage; and an almost linear function with a strongly saturated part when the amplitude of the input signal takes positive values. Adding a DC source can add unwanted energy lost.

According to our simulations, this circuit has a behavior similar to a low-pass filter with a very limited bandwidth and a significant gain loss, see Fig. 62. We were then confronted with the same problems as for the previous logarithmic circuit. Certainly, a better choice of different components of the circuit can improve the bandwidth, but the circuit will always suffer from its asymmetric transfer function not suitable for telecommunication signals. For all these reasons, we have decided to abandon this type of circuit.

C. EXPONENTIAL CIRCUIT

The exponential function $y(t) = \exp(-a|x(t)|)$ can be a good candidate for our application. Indeed, if the input signal is powerful, the output signal becomes too weak; in this case the effect of the strong signal is reduced to allow the extraction of the weaker signal. The developed circuit is presented in Fig. 63.

The introduction of a diode into a circuit with an operational amplifier allowed us to produce an exponential function of type $y(t) = \exp(-ax(t))$; i.e the input signal is assumed to be positive. This type of circuit suffers from the same disadvantages of the previous ''square root'' circuit. The input-output transfer function is shown in Fig. 66.

To check the asymmetric effect (no response for the negative part of the input signals), the linear gain for low amplitudes and the saturation for high amplitudes, we carry out simulations with various sinusoidal signals, see the Fig. 65.

Our simulations showed that the exponential function circuit has a bandpass filter behavior centered around 550 kHz with a low bandwidth of 30KHz, see Fig. 66.

D. BROADBAND CIRCUITS

In many modern applications such as tracking radar, electronic warfare, cognitive radio or electromagnetic surveillance, the receiver can be in close proximity to an unwanted transmitter. The unwanted transmitter may be authorized or unauthorized and may transmit intentionally or unintentionally in order to jam the receiver. The signal transmitted by this transmitter is considered unwanted and will be

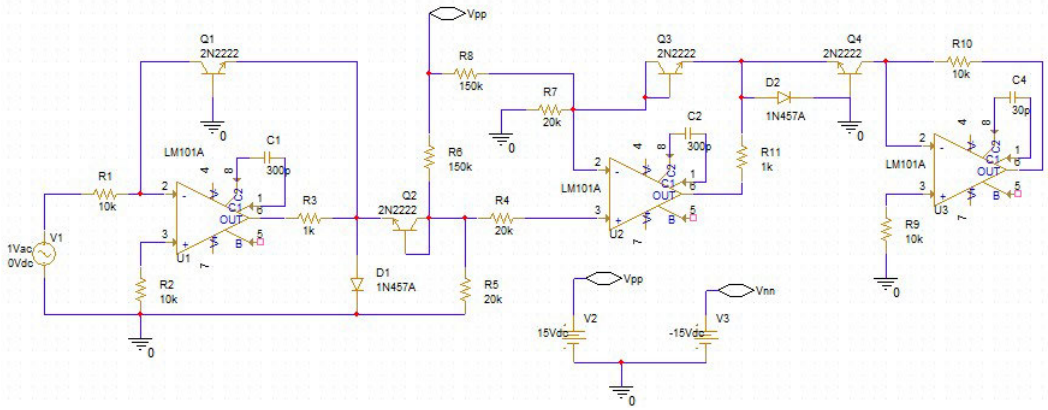

FIGURE 60. Simplified Square Root Circuit.

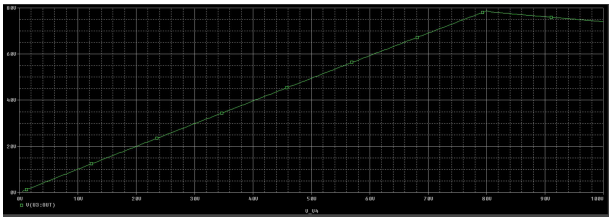

FIGURE 61. Simplified square root circuit bandwidth.

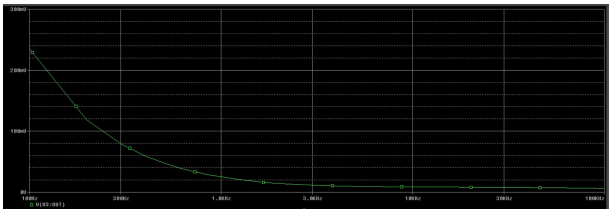

FIGURE 62. Simplified square root circuit bandwidth.

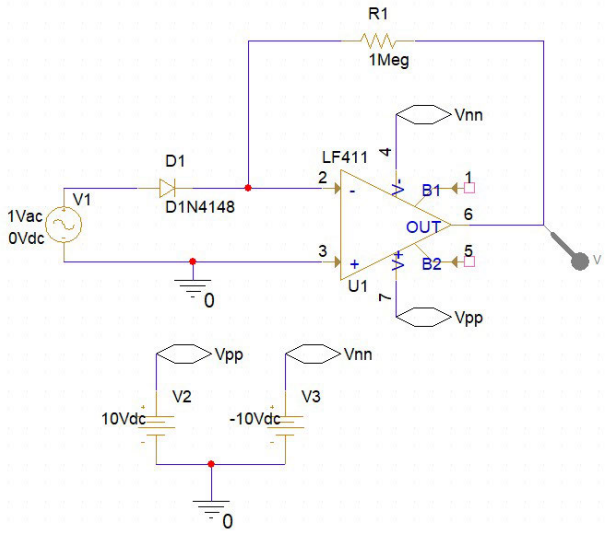

FIGURE 63. Exponential Circuit.

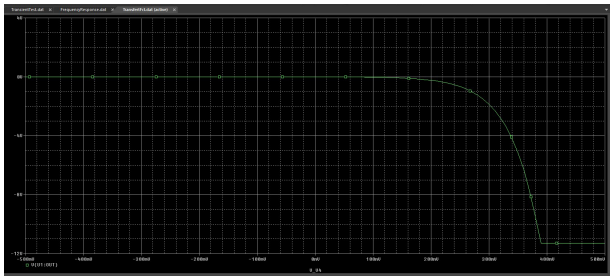

FIGURE 64. The temporal input-output transfer function.

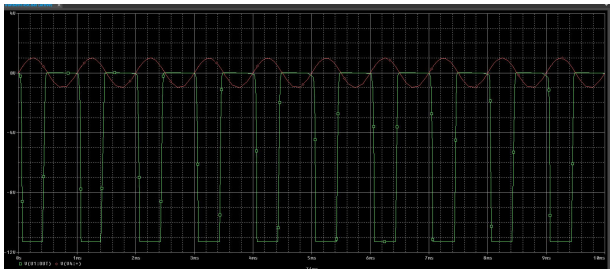

FIGURE 65. The non-linear effect of the circuit: the input signal is presented in red and the output signal in green.

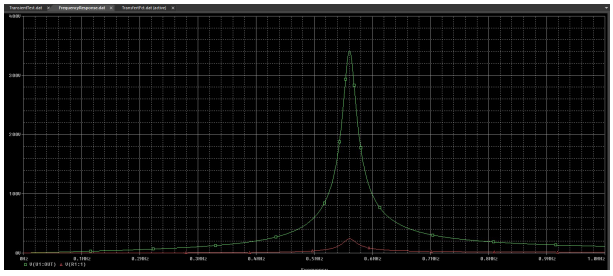

FIGURE 66. Bandwidth of the exponential function.

considered hereinafter as the jamming signal. In this case, the received signal results from a very strong spurious signal (the Jamming Signal) emitted by the nearby transmitter and a very weak target signal. In radio communication applications, authorized transmitters have limited transmission power. Even in this situation, the ratio between the jamming signal and the useful signal can exceed 80 dB. By definition, the

dynamic range (or range) of a system is the ratio between the smallest and largest amplitudes of signals that can be processed by that system.

A 14- to 16-bit analog-to-digital converter (ADC) [36] is commonly used in digital radio communications receivers. For such an ADC, the quantization step can be approximated as the ratio between the maximum input voltage and 2^n, where n represents the number of bits of the ADC. The quantization step characterizes the dynamic range of our receivers. Indeed, the maximum dynamic range (D_r) achievable in a digital system can be approximated by $D_r \approx 20\log(2^n) \approx 90dB$, when $n = 15$. In order to limit the dynamics of input signals, Automatic Gain Controllers (AGC) are conventionally introduced in many wireless receivers. However, AGC latency becomes a major disadvantage for these circuits in certain applications, such as Moving Target Indicator (MTI) devices. The dynamic range of AGC can also be considered a limitation for other applications: radars, fiber optic communications, and recent radio communications applications. It should be emphasized that the AGC can only adjust its gain for a single-component signal. In this case, the reference value of the AGC is normally the power of the single signal at reception.

To solve the dynamics problem, Woronocow and Corney [33] introduced a logarithmic amplifier based on two stages. The two stages were implemented using two different amplifiers, the first one is high gain with a low limit for the output voltage and the second one is unity gain and a high output voltage. Based on the circuits developed in [33], Loesch [37] developed another circuit to make a logarithmic amplifier with a dynamic range of 60dB. Its amplifier can operate around a frequency of 768MHz. The circuit proposed by Loesch contains Avantec UA404 type components. In the early 1980s, a circuit called the ''true logarithmic amplifier'' was introduced by Barber and Brown [31] to operate on the intermediate frequency (IF) of a radar. In their circuit, they used monolithic bipolar transistors. According to the authors, the logarithmic amplifier can filter a target signal from signals caused by raindrops (''Clutters''). As phase is important for MTI radars, the logarithmic amplifier was positioned on the IF stage of the receiver. It should be noted that the logarithmic amplifier proposed in [31] can process 70MHz signals with a dynamic range of 80 dB. By cascading six identical steps and using FET (Field Effect Transistor) transistors of the ''monolithic Gallium Arsenide Metal-Semiconductor'' (GaAs MESFET) type, Smith in [32] developed an integrated circuit in order to realize a logarithmic amplifier with a dynamic range of 70 dB. The major advantage of Smith's circuit compared to that of [31] is that the new circuit can cover a wide bandwidth between 500 MHz and 5 GHz. Holdenried et al. [38] developed a new ''true logarithmic amplifier'' using a parallel-summation topology. Their circuit has a lower dynamic range of 40 dB, however it has a wide bandwidth (DC-4GHz). Their low group delay distortion circuit is suitable for use in fiber optic or radar type applications with narrow pulses. In [39], Holdenried and Haslett proposed another circuit that covers larger bandwidth, DC-6 GHz; their new circuit uses heterogeneous bipolar transistors based on silicon-germanium (HBT SiGe, Silicon-Germanium Heterojunction Bipolar Transistors). These latter amplifiers use Cherry-Hooper gain stages with emitter follower feedback. In [40], the authors analyzed several solutions and simulated a variety of circuits in order to compare their performance. The circuits analyzed are AGC type, voltage controlled amplifiers (VCAS) and logarithmic amplifiers.

In our project, we aim for circuits with high dynamics (more than 100 dB) and the signals are assumed to be broadband signals (5 to 80MHz). Our device must be capable of processing very high frequency (VHF) signals (3 to 30 MHz), ultra high frequency (UHF) signals (300 MHz - 3 GHz) as well as in the WiFi band (at 2.4 GHz and at 5 GHz). In our study, several circuits were analyzed and simulated. The circuits mentioned above and other [41], [42], [43] technologies were also considered in our study.

1) MOSFET

A MOSFET transistor is another electronic component that can also be used to create a non-linear function. Indeed, such a transistor operates in two modes, the Drain-Source current relationship $i_D(t)$ as a function of the Drain-Source voltages $v_{DS}(t)$ and Gate-Source voltage $v_{GS}(t)$ [44]:

- Triode Region:

$$i_D(t) = k'_n \frac{W}{L}\left[(v_{GS} - V_t)v_{DS} - \frac{1}{2}v_{DS}^2\right] \tag{27}$$

- Saturation Region:

$$i_D(t) = k'_n \frac{1}{2}\frac{W}{L}(v_{GS} - V_t)^2 \tag{28}$$

with the transconductance parameter $k'_n = \mu_n C_{ox}$, the surface mobility μ_n, the unit capacitance $C_{OX} = \frac{\epsilon_{OX}}{t_{OX}}$, the permittivity $\epsilon_{OX} = 3.45 * 10^{-11}$ measured in Farad / meter (F/n), W is the width of the depletion channel, t_{OX} is the thickness of the oxide, and L represents the length of the depletion channel.

2) BIPOLAR TRANSISTOR

Another possible solution can be based on a bipolar transistor (Bipolar Junction Transistor, BJT), the current through the collector ''C'', in a saturation mode, can be approximated as follows [44]:

$$i_C \approx I_s \exp\left(\frac{v_{BE}}{V_T}\right) - \frac{I_s}{\alpha_R}\exp\left(\frac{v_{CB}}{V_T}\right) \tag{29}$$

where I_s is the saturation current which depends on the used materials and the dimensions of the BJT, V_T is the thermal voltage, α_R stands for the gain between the base and the collector, V_{CB} represents the voltage difference between the

collector and the base, and V_{BE} is the voltage difference between the base and the emitter.

According to [31], the diode-based technique is mainly used to design logarithmic amplifiers for applications with frequencies below 60 MHz.

3) MULTI-STAGE LOGARITHMIC AMPLIFIER

Woroncow and Croney in [33] proposed the first multi-stage logarithmic amplifier. The same technique has been used in real systems and has given good results at high frequency, [31], [38]. The "true logarithmic amplifier" is obtained by cascading N double gain stages. Each stage is composed of an operational amplifier mounted as a follower and another amplifier in parallel with a gain A, a saturation voltage at the input, V_{IL}, and a saturation voltage at the output $V_{OL} = AV_{IL}$.

The transfer function of each stage is given by the following equation:

$$V_{Out} = \begin{cases} (1+A)V_{in} & \text{si } |V_{in}| < |V_{IL}| \\ (|V_{in} + V_{OL}|)\text{Sgn}(V_{in}) & \text{ailleurs} \end{cases} \quad (30)$$

To create a "true logarithmic amplifier", the authors of [38] used MOSFET transistors in order to reach very high frequencies. In the proposed architecture, each stage contains four amplifiers. In our study, we simulated the structure of a "true logarithmic amplifier" using the circuit shown in Fig. 67. According to [31], the dynamics of this circuit is $(A+1)N$. To achieve a dynamic range of 70 dB, the circuit parameters can be adjusted as follows:

$$A = 3.0;\ V_{OL} = 0.764;\ \text{et } N = 6.$$

The value of V_{OL} was selected by a heuristic study. It should be noted that the amplifiers with a gain and a saturation function were made using two different circuits: an amplifier with a gain A followed by a limiting device. The limitation was achieved using two saturated amplifiers, as shown in Fig. 68.

4) LOGARITHMIC AMPLIFIERS WITH PARALLEL ADDITION TOPOLOGY

In [45], Yong et al. proposed a logarithmic amplifier with a parallel addition topology to create a reader of a RFID (Radio-frequency identification) card in the UHF (Ultra High Frequency) band. Holdenried et al. have made a "true logarithmic amplifier" that operates in the DC-4GHz band. The authors of [38] proposed two different topologies based on the structure of the "true logarithmic amplifier": A logarithmic amplifier using a "Progressive compression parallel-summation" topology; and another logarithmic amplifier based on a parallel-amplification and parallel-summation topology. According to [38], the transfer functions of two circuits are identical. The major difference between the two topologies consists of replacing a sequential addition circuit with another circuit with parallel addition.

The phase and group delay are relatively improved compared to other topologies. Let us denote by G_{pi} the gain of the ith stage and by G_j the total gain after stage i, $\forall 1 \leq j \leq N$, we can then write:

$$I_{Out} = \left(N + \log_A\left(\frac{g_m(A-1)V_{in}}{I_L A^2}\right) + \frac{A}{A-1}\right) I_L \quad (31)$$

Assuming that the gain of the first stage is $G_1 = G_{p1} = g_m$, the saturation amplifier of each stage also has the same gain g_m, and the other amplifiers have a gain equal to A, we can then conclude that $\forall 1 \leq j \leq N$:

$$G_j = g_m A^{j-1} \quad (32)$$

Using equations (31) and (32), the gains of different paths can be written as follows, $\forall 2 \leq i \leq N$:

$$G_{pi} = g_m A^{i-2}(A-1) \quad (33)$$

According to equation (33), we can conclude that, $\forall 1 \leq j \leq N$:

$$G_{pi} = g_m \prod_{i=1}^{j-1} G_{Ai} \quad (34)$$

The transfer function of this topology can be evaluated using an approach similar to that developed in the previous paragraph. Indeed, consider that the input signal V_{in} is small enough to pass through the first $(i-1)$ steps without triggering saturation. In this case, the amplitude of the input signal, V_{in}, is given by:

$$V_{in} = \frac{I_L}{G_{pi}} = \frac{I_L}{g_m A^{i-2}(A-1)} \quad (35)$$

$$\Longrightarrow\ i = \log_A\left(\frac{I_L A^2}{g_m(A-1)V_{in}}\right) \quad (36)$$

where I_L is the limiting current. As saturation is triggered at stage i, this means that all subsequent stages must also be saturated and the final current at the circuit output must be given by the following equation:

$$\begin{aligned} I_{Out} &= (N-i)I_L + G_i V_{in} \\ &= (N-i)I_L + \frac{G_i I_L}{G_{pi}} \\ &= (N-i)I_L + \frac{g_m A^{i-1} I_L}{g_m A^{i-2}(A-1)} \\ &= \left(N - i + \frac{A}{A-1}\right) I_L \end{aligned} \quad (37)$$

Using equations (36) and (37), we can conclude that:

$$G_j = \sum_{i=1}^{j} G_{pi} \quad (38)$$

According to [38], the main disadvantage of the progressive compression amplifier is that the phase delays of all channels are different. Using a Cherry-Hooper circuit for all gain stages, the authors of [39] modified the original design in order to obtain approximately the same delay on the different paths.

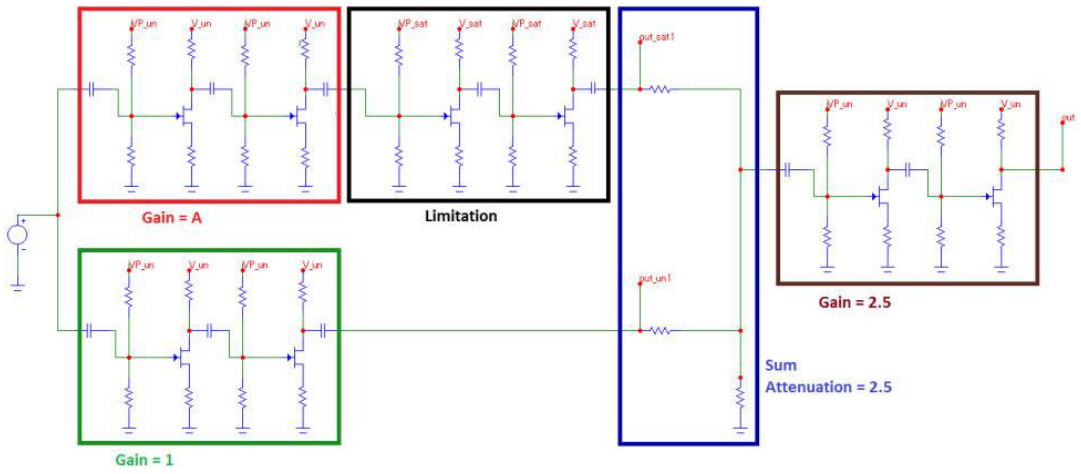

FIGURE 67. Simplified Square Root Circuit.

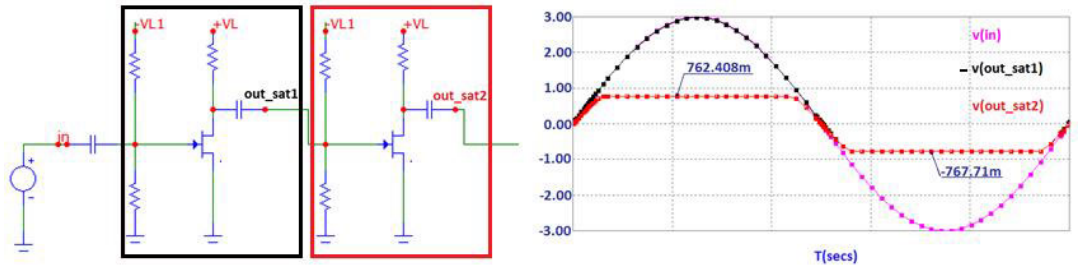

FIGURE 68. Characteristics of a stage: a) Limiting circuit & b) Saturated sinusoidal signal.

E. NON-LINEAR ANALOG-TO-DIGITAL CONVERTER

Analog-to-Digital Converters (ADCs) are essential components in all digital processing systems. ADCs are designed to convert arbitrary waveform analog signals to digital. These components are relatively expensive and energy intensive. However, to convert specific signals, certain aspects of the signal can help optimize the ADC design to achieve higher speed performance, power dissipation, or complexity. We have discussed several possibilities in previous sections to avoid the use of sophisticated and therefore expensive converters. Hereinafter, we provide a limited but consistent state of the art on the architectures used in the design of linear (classic) or non-linear analog-to-digital converters [46], [47], [48], [49], [50], [51], [52].

Depending on application and the specific cases, different types of nonlinearity functions are employed in nonlinear ADCs, including [46] and [48]: the exponential function, the logarithmic function, the piecewise linear approximation of the logarithmic function, and a non-uniform staircase.

Hereinafter, we introduce the classic design architectures of ADCs, then we introduce more recent non-linear ADCs which can in theory be used in our reception chain to replace both the analog circuit of the bijective nonlinear function and a classical ADC. It must be emphasized that the results of this section remain within the framework of a bibliographic study. Indeed, the validation of these circuits within the framework of our study requires the acquisition of these circuits, as well as the practical experimentation platform. This is outside the scope of our preliminary and proof-of-concept study.

Logarithmic digital analog converters are widely used in communications, instrumentation and hearing aids, among other application areas, where it is necessary to match the dynamics of the signals to the dynamics of the transmission channels. Originally, logarithmic converters were implemented in bipolar technology to explore the exponential I-V characteristic of transistors [47].

In this paper, two new types of logarithmic analog-to-digital converter suitable for high frequency applications have been introduced. While the logarithmic operation is obtained by replacing the linear operations of subtraction with division and multiplication by 2 with a square operation. The two new logarithmic A/D converters are based on the architecture of a two-stage flash ADC or pipeline architecture suitable for the application of CMOS technology.

1) TWO-STAGE FLASH LOGARITHMIC ADC

In [50], they illustrates the operating principle of a classic linear ADC with a two-stage flash architecture. During the quantization cycle, the first flash converter quantizes a sampled input and keeps it constant during the sampling period (at the output of the S/H: Sample and Hold Circuit block). In addition, a reconstructed voltage corresponding to

the N secondary bits is subtracted from the sampled input (S/H) in order to generate a residual voltage. This last voltage is amplified by 2^N then it is applied to the second flash converter to extract least significant bits.

For the realization of a two-stage logarithmic ADC, the operations used in the classic ADC must be performed in the logarithmic domain [50], where the subtraction is equivalent to a division, and multiplication to addition. Such a transformation can be obtained by considering the input voltage V_{in} as an exponential function of the digital value D desired at the output:

$$V_{in} = K \exp\left(D \frac{\ln\left(\frac{1+K}{K}\right)}{2^N}\right) \tag{39}$$

where N represents the resolution level and K is a normalization constant to obtain a full scale input voltage range of 1 V. input voltage ($V_{ref} = 0.1986$) which is the center of the input voltage in a logarithmic scale.

Logarithmic converters must follow a logarithmic quantization law to extract both the low and high bits. The first ADC extracts the most significant bits (in logarithmic scale) which control ADC. In the linear case, the output of ADC is subtracted from the input; while in the logarithmic domain, where subtraction is equivalent to a division, this operation corresponds to an attenuation dependent on the digital word at the input of ADC, [51]. In the latter case, the ADC should be replaced by a logarithmic attenuator digitally controlled whose attenuation factor is given by:

$$a_n = \exp\left(\frac{\ln\left(\frac{1+K}{K}\right)}{2^{(N-N_2)}} n\right) \tag{40}$$

where $n \in [0, 2^{N_1} - 1]$, N_1 and N_2 are respectively the resolution bits of the first and 2nd flash converters. In order to implement logarithmic operations, Guilherme et al. [51] proposed a logarithmic architecture.

2) LOGARITHMIC ADC WITH PIPELINE ARCHITECTURE

The functional diagram of a linear ADC with pipeline architecture is proposed in [28]. In each stage and depending on the comparator output, the reference voltage V_{ref} will be (or not) subtracted from the input signal and then multiplied by two. Obtaining a logarithmic ADC with pipeline architecture can be obtained by performing the operations in the logarithmic domain, where subtraction is equivalent to division, and the multiplication by two is equivalent to the square of the signal.

In a similar way to the multi-stage ADC presented in the previous section, the authors of [52] propose to consider an input voltage V_{in} as an exponential function of the value digital D desired at the output:

$$V_{in} = \exp\left(D \frac{\ln\left(V_{inmax}\right)}{2^N}\right) \tag{41}$$

where N represents the resolution level and V_{inmax} is the maximum value at the input.

The most significant bit, b_6, is obtained by comparing the input voltage V_{in} with V_{ref}: If $V_{in} < V_{ref} \Longrightarrow b_6 = 0$ and V_{in} remains unchanged; otherwise $b_6 = 1$ and we must subtract V_{ref} from V_{in}. In a logarithmic scale, and using $V_{ref} = \sqrt{2}$, the subtraction (V_{ref} from V_{in}) is equivalent to the following operation:

$$V_{new} = \frac{V_{in}}{\sqrt{2}} \tag{42}$$

In both cases, the signal obtained is then multiplied by two which corresponds in the logarithmic scale to square of the signal. By generalizing this approach, the authors of [52] proposed a logarithmic ADC with pipeline architecture.

The realization of the square function is difficult to be implemented in an integrated circuit. To overcome this difficulty, Guilherme et al. [52] proposed another architecture. In the new architecture, the reference voltages of each stage were calculated from the reference voltage of the previous stage.

VI. DISCUSSION

At first, we would like to highlight that many simulation software have been used in our project. However, all figures shown in our manuscript have been obtained through PsPice simulations and Matlab.

A. A BRIEF COMPARISON BETWEEN THE PROPOSED SCHEME AND TRADITIONAL SOLUTIONS

To our knowledge, most traditional receivers use high-order filters to receive weak signals. The results can be significantly affected by the nature of the selected filter, its order, and the technology used to realize the filter. In many cases, we may encounter problems related to the use of such filters. Indeed, an active filter may be limited in its bandwidth, while a passive one can significantly affect the energy of the received signal. Furthermore, if the weak signal is close to a strong interfering signal, the filter solution (which is not flexible enough to adapt to operational scenarios involving dynamic signals) may fail to protect the target weak signal due to the actions of other parts of the receiver (mainly the AGC, LNA, and ADC). In such scenarios, our proposed solution can be useful for the following reasons:

1) It is easier to implement than a high-order dynamic active filter.
2) It can cover a large bandwidth.
3) Even with weak SINRs, the proposed solution can successfully detect the presence of a weak target signal, as demonstrated in our simulations.

The drawbacks of the proposed solution can be influenced by the choice of the non-linear function:

1) The mathematical properties of the non-linear function and its inverse can affect the overall performance of the system. In our study, we provided a proof of concept

and obtained promising results with certain non-linear functions. Another part of this study can focus on the choice of an optimal function, where the selected optimization criteria should be suitable for a target application. Such a study is very interesting but is beyond the scope of the current proposed study and can be considered in our future work.

2) The choice of a non-linear function should be strongly related to the analog electronic circuit. In other words, the optimization proposed in the previous point should be undertaken with respect to technological and physical constraints.
3) The selected non-linear function should have a stable and low computational cost inverse digital function.
4) In our study, we only considered a limited number of available electronic circuits and components. This part of our study can also be extended to consider new advanced electronic components and circuits.

Based on the above reasons, we conclude that the proposed solution can detect weak signals where classical solutions may fail. However, the proposed architecture should focus on the operational scenario followed by an optimization study with the help of more advanced technological circuits.

B. CONSEQUENCES OF ADDING THE PROPOSED SCHEME TO CLASSIC RECEIVERS

The proposed scheme necessitates modifications to both the analog and digital parts of the receiver. These modifications raise several important considerations:

1) Analog-Digital Matching: The perfect matching between the analog non-linear bijective function, implemented using electronic components (which may suffer from hardware limitations), and its digital inverse function can affect overall performance.
2) Increased Complexity: The proposed scheme slightly increases the complexity of the receiver.
3) Residual Non-Linear Effects: Residual non-linear effects in the output signal may affect transmission quality.
4) Quality Alterations with Complex Functions: Highly complex non-linear functions may alter the quality of intercepted signals, potentially increasing the Bit Error Rate (BER).
5) Detection of Weak Signals: Despite these challenges, the proposed scheme can detect weak signals that would otherwise be undetectable.
6) Adaptive Filtering: Based on its detection capabilities, the proposed scheme can initially be used to detect, characterize, and identify intercepted weak signals. Subsequently, the obtained information can be used to tune an adaptive filter for better extraction of the intercepted signal.

VII. CONCLUSION

In recent radio applications, receivers can be affected by high-power jamming signals. In this case, the received signal can be considered as the sum of a strong interfering signal and a very weak target signal. The ratio of the powers of these two signals (interfering and useful) characterizes the dynamics of the system to be created. Even if the two signals do not overlap in the frequency domain, the reception of the weak signal becomes very difficult because it can disappear at the output of the analog-to-digital converter. The nature of wideband signals with very close frequency bands creates a challenge for the interception of analog signals. To avoid this scenario, we may use hyper-selective RF analog filters with a very high order. This solution does not constitute a practically feasible solution, especially to cover a wide frequency band and a fairly large dynamic range. This solution becomes even more complicated in an interception scenario. On the other hand, a high order digital filter can be implemented. The use of such a filter requires that the signals can be properly converted to digital signals by our processing chain. This involves the use of a high resolution analog to digital converter, this type of converter involves two problems: the used technology and the price. Our study focuses on the separation of a weak target signal and a very strong interfering signal which are broadband signals with adjacent frequency bands.

To avoid the use of a very selective RF filter or a sophisticated and therefore expensive ADC, we proposed a solution based on the introduction into the reception chain of two additional modules:

- An analog circuit carrying out a non-linear limiting but bijective and therefore invertible function.
- An inverse numeric function.

In our study, several non-linear functions were studied: Square Root, Exponential, Logarithmic, etc. Several circuits were implemented and simulated. Some circuits have been modified, new diagrams have been proposed and also presented. Our study is structured around the following axis:

- Non-linear and simple amplifier: The main goal of this part is concept validation. The considered circuits studied are deliberately chosen to be simple and easy to simulate. Once the concept was validated, the limits concerning the frequency band or the dynamic range of these circuits are highlighted. To reduce the limitations of our circuits, the search for other circuits is imposed. Finally, this part helped us define our needs and the essential areas of research to approach the rest of our studies.
- Multi-stage logarithmic amplifier: The analyzed and simulated circuits are based on real circuits proposed to solve problems linked to certain radar applications. The results of our simulations showed the effectiveness of these circuits and the validation of our complete reception chain. Having proven the existence of a practical solution through the studies carried out in

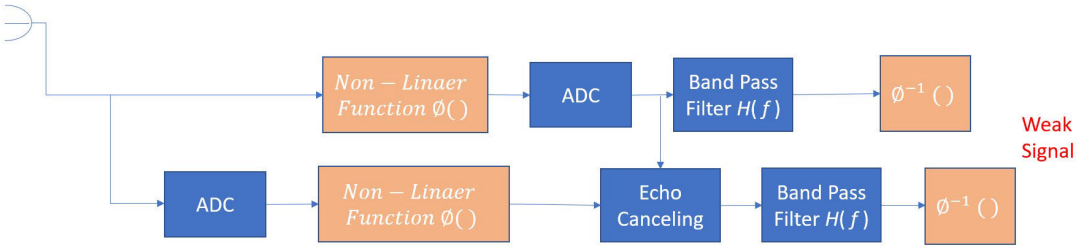

FIGURE 69. A possible extension to the non-linear system.

this part, our main challenge becomes the extension of the limits of the proposed circuits. This extension is studied in order to analyze several non-linear functions.

- Various circuits with non-linear transfer functions: In this part, we analyzed, tested or developed several non-linear amplifiers, and we obtained good results. Finally, the simulations are presented and discussed.
- Non-linear analog-to-digital converters: We limited ourselves to bibliographic studies. The main objective was to explore the literature in order to look for original solutions or compact circuits performing both the non-linear analog function and the analog-to-digital converter.

We can notice that the proposed solution doesn't affect the main digital part of the demodulator, see Figures 3 and 4. Therefore, the proposed solution can be theoretically (except for the matching problem discussed in previous section). From this point of view, the proposed solution has very nice scalability and flexibility properties, and it may be implemented in many wireless devices. Besides, the proposed solution introduces only two parts at the receiver side, so we are completely operating in a passive mode. Therefore, we will not be concerned by any legal issues. However, the introduction of nonlinear component in the receiver side can affect the quality of the received signal as it was discussed in previous section.

The natural extension of this study must mainly address the following points:

1) Study and simulation of component imperfections especially in multi-stage logarithmic amplifiers.
2) Study and simulation of overall error rate between the transmitter and the receiver.
3) Integration of digital algorithms into the complete processing chain.
4) Validation of simulated circuits on prototype circuits.
5) Integration of new components that have recently been introduced to the market but also to simulation software.
6) Consideration of thermal noise and parasitic sources in the various components used.
7) Consideration of the microwave effects of the various circuits.
8) Testing circuits in a real scenario.
9) We could also aim for an extension of the system proposed in this study by another system which will be more effective by introducing echo cancellation techniques "Echo Canceling". The proposed architecture is presented in Fig. 69.

REFERENCES

[1] P. B. Kenington and L. Astier, "Power consumption of A/D converters for software radio applications," *IEEE Trans. Veh. Technol.*, vol. 49, no. 2, pp. 643–650, Mar. 2000.
[2] E. E. Azzouz and A. K. Nandi, *Automatic Modulation Recognition of Communication Signals*. Norwell, MA, USA: Kluwer Academic Publishers, 1996.
[3] D. Le Guen and A. Mansour, "Automatic recognition algorithm for digitally modulated signals," in *Proc. IASTED Int. Conf. Signal Process., Pattern Recognit., Appl.*, 2002, pp. 25–28.
[4] K. N. Haq, A. Mansour, and S. Nordham, "Comparison of digital modulation classification based on statistical approaches," in *Proc. The 10th Postgraduate Electr. Eng. Comput. Symp.*, Oct. 2009, pp. 1–12.
[5] S. Pinet, "Etude et reconnaissance de signaux à modulations numériques rapides à partir de transformations temps-fréquence," Ph.D. dissertation, Faculté des Sci., Universite de Nice-Sophia Antipolis, Nice, France, 1995.
[6] D. Le Guen and A. Mansour, "Automatic recognition algorithm for digitally modulated signals," in *Proc. 6th Baiona Workshop Signal Process. Commun.*, 2003, pp. 25–28.
[7] K. N. Haq, A. Mansour, and S. Nordholm, "Classification of digital modulated signals based on time frequency representation," in *Proc. 4th Int. Conf. Signal Process. Commun. Syst.*, Dec. 2010, pp. 1–5.
[8] K. Nadya Haq, A. Mansour, and S. Nordholm, "Recognition of digital modulated signals based on statistical parameters," in *Proc. 4th IEEE Int. Conf. Digit. Ecosystems Technol.*, Apr. 2010, pp. 565–570.
[9] M. Pedzisz and A. Mansour, "HOS-based multi-component frequency estimation," in *Proc. 13th Eur. Signal Process. Conf.*, Sep. 2005, pp. 1–4.
[10] M. Pedzisz and A. Mansour, "Automatic modulation recognition of MPSK signals using constellation rotation and its 4th order cumulant," *Digit. Signal Process.*, vol. 15, no. 3, pp. 295–304, May 2005.
[11] L. W. Couch, *Digital and Analog Communication Systems*. Upper Saddle River, NJ, USA: Prentice-Hall, 2001.
[12] S. Haykin and M. Moher, *Communication Systems*. Hoboken, NJ, USA: Wiley, 2009.
[13] J. Proakis and M. Salehi, *Digital Communications*. New York, NY, USA: McGraw-Hill, 2007.
[14] A. Mansour, R. Mesleh, and M. Abaza, "New challenges in wireless and free space optical communications," *Opt. Lasers Eng.*, vol. 89, pp. 95–108, Feb. 2017, doi: 10.1016/j.optlaseng.2016.03.027.
[15] A. Graham, *Communications, Radar and Electronic Warfare*. Hoboken, NJ, USA: Wiley, 2011.
[16] Z. Ghassemlooy and W. O. Popoola, *Mobile and Wireless Communications Network Layer and Circuit Level Design*. Chennai, India: InTech, Jan. 2010, pp. 355–392.
[17] V. Madisetti, *The Digital Signal Processing Handbook: Wireless, Networking, Radar, Sensor Array, Processing, and Nonlinear Signal Processing*. Boca Raton, FL, USA: CRC Press, 2010.
[18] J. Proakis and M. Salehi, *Fundamentals of Communication Systems*. London, U.K.: Pearson, 2015.

[19] S. Haykin, *Digital Communication Systems*. Hoboken, NJ, USA: Wiley, 2013.
[20] A. Quinquis, A. Mansour, and E. Radoi, *Signaux Et Systemes: Signaux, Filtrage Et Décision*. Paris, France: Hermes, Mar. 2019.
[21] C. Ioana, A. Mansour, A. Quinquis, and E. Radoi, *Digital Signal Processing Using MATLAB*. Hoboken, NJ, USA: Wiley, 2008.
[22] J. Proakis and M. Salehi, *Contemporary Communication Systems Using MATLAB* (Bookware Companion Series). New York, NY, USA: CL Engineering, 1998.
[23] M. G. Di Benedetto, T. Kaiser, A. F. Molisch, I. Oppermann, C. Politano, and D. Porcino, *UWD Communication Systems: A Comprehensive Overview*. Belgium, Europe: EURASIP, 2006.
[24] D. Battle, P. Gerstoft, A. Kuperman, W. Hodgkiss, and M. Siderius, *Multi-Band OFDM Physical Layer Proposal for IEEE 802.15 Task Group 3A*, document IEEE P802.15, 2004.
[25] G. Acosta. (2000). *Ofdm Simulation Using MATLAB*. [Online]. Available: http://www.ece.gatech.edu/research/labs/sarl/tutorials/OFDM/Tutorial-web.pdf
[26] L. Bin, T. W. Rondeau, J. H. Reed, and C. W. Bostian, "Analog-to-digital converters," *IEEE Signal Process. Mag.*, vol. 22, no. 6, pp. 69–77, Nov. 2005.
[27] A. M. A. Ali, A. Morgan, C. Dillon, G. Patterson, S. Puckett, P. Bhoraskar, H. Dinc, M. Hensley, R. Stop, S. Bardsley, D. Lattimore, J. Bray, C. Speir, and R. Sneed, "A 16-bit 250-MS/s IF sampling pipelined ADC with background calibration," *IEEE J. Solid-State Circuits*, vol. 45, no. 12, pp. 2602–2612, Dec. 2010.
[28] R. J. Van De Plassche, *CMOS Integrated Analog-to-Digital and Digital-to-Analog Converters*. Springer, 2003.
[29] F. Cottet, *Traitement Des Signaux Et Acquisition De Donnees*. Paris, France: Dunod, 2009.
[30] C. D. Holdenried, "A logarithmic amplifier and Hilbert transformer for optical single sideband," Ph.D. dissertation, Dept. Elect. Comput. Eng., Univ. Calgary, Calgary, Calgary, 2005.
[31] W. L. Barber and E. R. Brown, "A true logarithmic amplifier for radar if applications," *IEEE J. Solid-State Circuits*, vols. SC-15, no. 3, pp. 291–295, Jun. 1980.
[32] M. A. Smith, "A 0.5 to 4 GHz true logarithmic amplifier utilizing monolithic GaAs MESFET technology," *IEEE Trans. Microwave Theory Techn.*, vols. MTT-36, no. 12, pp. 1986–1990, Dec. 1988.
[33] A. Woroncow and J. Corney, "A true logarithmic amplifier using twin-gain stages," *Radio Electron. Engineer*, vol. 1, pp. 149–155, Sep. 1966.
[34] R. J. Widlar. (2007). *Root Extractor*. [Online]. Available: http://www.freecircuits.net/circuit-46.html
[35] K. Murao, T. Kohda, K. Noda, and M. Yanase, "1/f noise generator using logarithmic and antilogarithmic amplifiers," *IEEE Trans. Circuits Syst.*, vol. 39, no. 10, pp. 851–853, Oct. 1992.
[36] J. A. Wepman, "Analog-to-digital converters and their applications in radio receivers," *IEEE Commun. Mag.*, vol. 33, no. 5, pp. 39–45, May 1995.
[37] B. Loesch, "A UHF true logarithmic IF amplifier," *IEEE Trans. Aerosp. Electron. Syst.*, vol. AES-9, no. 5, pp. 660–664, Sep. 1973.
[38] C. D. Holdenried, J. W. Haslett, J. G. McRory, R. D. Beards, and A. J. Bergsma, "A DC-4-GHz true logarithmic amplifier: Theory and implementation," *IEEE J. Solid-State Circuits*, vol. 37, no. 10, pp. 1290–1299, Oct. 2002.
[39] C. D. Holdenried and J. W. Haslett, "A DC-6 GHz, 50 dB dynamic range, SiGe HBT true logarithmic amplifier," in *Proc. IEEE Int. Symp. Circuits Syst.*, Oct. 2004, pp. 289–292.
[40] W. Kester, J. Bryant, B. Clarke, and B. Gilbert. (1996). *Rf/IF Subsystems*. [Online]. Available: http://www.analog.com/media/en/training-seminars/design-handbooks/366984825031162274991154371192sect3.pdf
[41] *Gallium Arsenide Phemt Rf Power Field Effect Transistor*, document MRFG35003N6AT1, 2009.
[42] *0.5–6 GHz Low Noise Gallium Arsenide Fet*, Hewlett Packard, Palo Alto, CA, USA, 1998.
[43] *Theory and Applications of Logarithmic Amplifiers*, document SNOA575B, 2013.
[44] A. S. Sedra and K. C. Smith, *Microelectronic Circuits*. New York, NY, USA: Oxford, 2014.
[45] Z. Yong, C. Lei, Z. Xiao-jun, and L. Zong-sheng, "A parallel-amplification parallel-summation logarithmic amplifier for UHF RFID reader," in *Proc. IEEE 8th Int. Conf. ASIC*, Changsha, China, Oct. 2009, pp. 1121–1124.
[46] H. Kunz, "Exponential D/A converter with a dynamic range of eight decades," *IEEE Trans. Circuits Syst.*, vols. CS-25, no. 7, pp. 522–526, Jul. 1978.
[47] B. Gottschalk, "Logarithmic analog-to-digital converter using switched attenuators," *Rev. Scientific Instrum.*, vol. 49, no. 2, pp. 200–204, Feb. 1978.
[48] J. N. Lygouras, "Nonlinear ADC with digitally selectable quantizing characteristic," *IEEE Trans. Nucl. Sci.*, vols. TNS-35, no. 5, pp. 1088–1091, Oct. 1988.
[49] Y. P. Tsividis, V. Gopinathan, and L. Toth, "Companding in signal processing," *Electron. Lett.*, vol. 26, no. 17, p. 1331, 1990.
[50] J. Guilherme and J. E. Franca, "Digitally-controlled analogue signal processing and conversion techniques employing a logarithmic building block," in *Proc. IEEE Int. Symp. Circuits Syst.*, May 1994, pp. 377–380.
[51] J. Guilherme and J. E. Franca, "A logarithmic digital-analog converter for digital CMOS technology," in *Proc. Asia–Pacific Conf. Circuits Syst.*, 1994, pp. 490–493.
[52] J. Guilherme and J. E. Franca, "New CMOS logarithmic A/D converters employing pipeline and algorithmic architectures," in *Proc. Int. Symp. Circuits Syst.*, 1995, pp. 529–532.

ALI MANSOUR (Senior Member, IEEE) received the M.Sc. and Ph.D. degrees from INPG, France, and the H.D.R. (Habilitation a Diriger des Recherches) degree from UBO, France. He held many positions: a Postdoctoral Researcher with LTIRF, France, a Researcher with RIKEN-Japan, a Teacher-Researcher with ENSIETA, France, a Senior Lecturer with Curtin Uni-Australia, an Invited Professor with ULCO, France, and a Professor with Tabuk Uni-KSA and ENSTA-Bretagne-France. He has published about 300-refereed publications in international journals or conferences. In addition, he is the author of a book and the co-author of four other books and ten book chapters and co-editor of two books. During his career, he had successfully supervised several postdoctoral, Ph.D. candidates, and M.Sc. students. He was the Vice President of IEEE Signal Processing Society in Western Australia for two years. He has also been a Lead Guest Editor of the *EURASIP Journal on Advances in Signal Processing* and a Lead Guest Editor for a special issue of sensors a MDPI journal. His research interests include source separation, high order statistics, signal processing, robotics, telecommunication, biomedical engineering, electronic warfare, and cognitive radio.

CHRISTOPHE OSSWALD received the Engineering degree in computer science from Telecom Bretagne (now part of IMT Atlantique), in 1999, and the Ph.D. degree from EHESS, in 2003. He is currently an Engineer with the Ecole Polytechnique. Since 2004, he has been an Assistant Professor with ENSTA Bretagne (formerly ENSIETA), teaching applied mathematics and computer sciences. He is also in charge of the Mathematics, Algorithms and Decision Thematic Group. His research interests include computational complexity, graph theory, unsupervised classification, belief functions, and game theory. He is a member of Lab-Sticc (UMR 6285).